
Deep ReLU Networks Have Surprisingly Simple Polytopes

Feng-Lei Fan*

Department of Mathematics
The Chinese University of Hong Kong
fengleifan@cuhk.edu.hk

Wei Huang

RIKEN AIP
weihuang.uts@gmail.com

Xiangru Zhong

Sun Yat-Sen University
zhongxr9@mail2.sysu.edu.cn

Lecheng Ruan

BIGAI

Tieyong Zeng

Department of Mathematics
The Chinese University of Hong Kong

Huan Xiong*

Institute for Advanced Study in Mathematics
Harbin Institute of Technology
huan.xiong.math@gmail.com

Fei Wang

Weill Cornell Medicine
Cornell University
few2001@med.cornell.edu

Abstract

A ReLU network is a piecewise linear function over polytopes. Figuring out the properties of such polytopes is of fundamental importance for the research and development of neural networks. So far, either theoretical or empirical studies on polytopes only stay at the level of counting their number, which is far from a complete characterization of polytopes. To upgrade the characterization to a new level, here we propose to study the shapes of polytopes via the number of simplices obtained by triangulating the polytope. Then, by computing and analyzing the histogram of simplices across polytopes, we find that a ReLU network has relatively simple polytopes under both initialization and gradient descent, although these polytopes theoretically can be rather diverse and complicated. This finding can be appreciated as a novel implicit bias. Next, we use nontrivial combinatorial derivation to theoretically explain why adding depth does not create a more complicated polytope by bounding the average number of faces of polytopes with a function of the dimensionality. Our results concretely reveal what kind of simple functions a network learns and its space partition property. Also, by characterizing the shape of polytopes, the number of simplices be a leverage for other problems, *e.g.*, serving as a generic functional complexity measure to explain the power of popular shortcut networks such as ResNet and analyzing the impact of different regularization strategies on a network's space partition.

1 Introduction

It was shown in a thread of studies Chu et al. [2018], Balestriero and Baraniuk [2020], Hanin and Rolnick [2019b], Schonsheck et al. [2019] that a neural network with the piecewise linear activation is to partition the input space into many convex regions, mathematically referred to as polytopes, and each polytope is associated with a linear function (hereafter, we use convex regions, linear regions, and polytopes interchangeably). Hence, a neural network is essentially a piecewise linear function over polytopes. Based on this adorable result, the core idea of a variety of important

*Corresponding author.

theoretical advances and empirical findings is to turn the investigation of neural networks into the investigation of polytopes. Figuring out the properties of such polytopes can shed light on many critical problems, which can greatly expedite the research and development of neural networks. Let us use two representative examples to demonstrate the utility of characterizing polytopes:

The first representative example is the explanation of the power of depth. In the era of deep learning, many studies [Mohri et al., 2018, Bianchini and Scarselli, 2014, Telgarsky, 2015, Arora et al., 2016] attempted to explain why a deep network can perform superbly over a shallow one. One explanation to this question is on the superior representation power of deep networks, *i.e.*, a deep network can express a more complicated function but a shallow one with a similar size cannot [Cohen et al., 2016, Poole et al., 2016, Xiong et al., 2020]. Their basic idea is to characterize the complexity of the function expressed by a neural network, thereby demonstrating that increasing depth can greatly maximize such a complexity measure compared to increasing width. Currently, the number of linear regions is one of the most popular complexity measures because it respects the functional structure of the widely-used ReLU networks. Pascanu et al. [2013] firstly proposed to use the number of linear regions as the complexity measure. By directly applying Zaslavsky’s Theorem [Zaslavsky, 1997], Pascanu et al. [2013] obtained a lower bound $\left(\prod_{l=0}^{L-1} \left\lfloor \frac{n_l}{n_0} \right\rfloor\right) \sum_{i=0}^{n_0} \binom{n_l}{i}$ for the maximum number of linear regions of a fully-connected ReLU network with n_0 inputs and L hidden layers of widths n_1, n_2, \dots, n_L . Since this work, deriving the lower and upper bounds of the maximum number of linear regions becomes a hot topic [Montufar et al., 2014, Telgarsky, 2015, Montúfar, 2017, Serra et al., 2018, Croce et al., 2019, Hu and Zhang, 2018, Xiong et al., 2020]. All these bounds suggest the expressive ability of depth. The second interesting example is the finding of the high-capacity-low-reality phenomenon [Hu et al., 2021, Hanin and Rolnick, 2019b], that the theoretical tight upper bound for the number of polytopes is much larger than what is actually learned by a network, *i.e.*, deep ReLU networks have surprisingly few polytopes both at initialization and throughout the training. This counter-intuitive phenomenon can also be regarded as an implicit bias, which to some extent suggests why a deep network does not overfit.

We observe that the current studies on polytopes suffer a critical limit. So far, either theoretical or empirical studies only stay at the level of counting the number of polytopes, which is far from a complete characterization of polytopes and the corresponding ReLU network. As we know, in a feed-forward network of L hidden layers, each polytope is encompassed by a group of hyperplanes, as shown in Figure 1(a), and each hyperplane is associated with a neuron. The details of how polytopes are formed in a ReLU network are in Appendix A. Hence, any polytope is created by at most $\sum_{i=1}^L n_i$ and at least $n_0 + 1$ hyperplanes, which is quite a large range. Thus, face numbers of polytopes can vary a lot. Unfortunately, the existing “counting” studies did not accommodate the differences among polytopes. *Can we upgrade the characterization of polytopes beyond counting to capture a more complete picture of a neural network?*

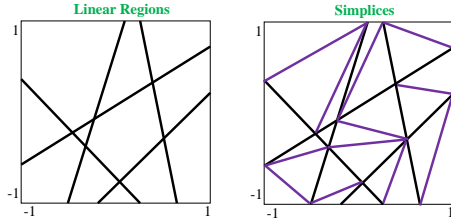


Figure 1: The number of simplices a polytope contains can reveal the shape information of a polytope, with which one can dig out valuable information of a neural network.

In this manuscript, 1) we propose to move one step further to study the shape of polytopes by seamlessly dividing each polytope into simplices in a triangulation of the polytope, as Figure 1(b) shows, and we describe the shape of polytopes by the minimum number of simplices to partition it. 2) We observe that polytopes formed by ReLU networks are surprisingly simple under both initialization and gradient descent, which is a fundamental characteristic of a ReLU network. Here, simplicity means that although theoretically quite diverse and complicated polytopes can be derived, deep networks tend to find a function with many simple polytopes. In addition, we underscore that the purported simplicity is relative to the possibly most complicated polytopes by a network in a given dimension. We do not compare polytopes in different input dimensions. Our results concretely reveal what kind of simple functions a network learns and its space partition property, which can be regarded as an implicit simplicity bias, explaining why deep networks may not overfit. 3) We establish a theorem that bounds the average face numbers of polytopes of a network to a small number. This theorem explains why depth does not make polytopes more complicated. The key idea is that increasing depth is to cut the existing polytope with a new hyperplane that cannot intersect with all faces of the existing polytope. Hence, the number of newly-generated faces is smaller than the current, and the average face number will not increase. To summarize, our contributions are threefold.

1. We point out the limitation of counting #polytopes. To deepen our understanding of how a ReLU network partitions the space, we propose to investigate the shape of polytopes with the minimum number of simplices to partition it. Investigating polytopes of a network can lead to a more complete characterization of ReLU networks.
2. We empirically find that a ReLU network has surprisingly simple polytopes under both initialization and gradient descent. Such an interesting finding is a new implicit bias from the perspective of shapes of linear regions. Previously, Hanin and Rolnick [2019b] showed that deep ReLU networks have few polytopes. Our discovery is that polytopes are simple, which is more fine-grained. *Our result and Hanin and Rolnick [2019b] address two essentially different aspects: quantity and shape.* Compared to [Hanin and Rolnick, 2019b], our result more convincingly illustrates a deep network learns a simple function. Showing the number of polytopes is few is insufficient to claim that a network learns a simple solution because a network can have a small number of very complicated polytopes.
3. To substantiate our empirical finding, we use combinatorial techniques to derive a tight upper bound for the average face number of polytopes, which not only offers a theoretical guarantee but also explains why increasing depth does not make polytopes more complicated.

2 Related Work

Studies on polytopes of a neural network. Besides the aforementioned works [Pascanu et al., 2013, Xiong et al., 2020, Montufar et al., 2014, Hu and Zhang, 2018] that count the number of polytopes, there are increasingly many studies on polytopes of neural networks. Chu et al. [2018], Hanin and Rolnick [2019b], Balestrierio and Baraniuk [2020] showed that polytopes created by a network are convex. Zhang and Wu [2020] studied how different optimization techniques influence the local properties of polytopes, such as the inspheres, the directions of the corresponding hyperplanes, and the relevance of the surrounding regions. Gamba et al. [2020] showed that the angles between activation hyperplanes defined by convolutional layers are prone to be similar after training. Hu et al. [2020] studied the network using an arbitrary activation function. They first used a piecewise linear function to approximate the given activation function. Then, they monitored the change of #polytopes to probe if the network overfits. Park et al. [2021] proposed neural activation coding that maximizes the number of linear regions to enhance the model’s performance. Our work goes beyond counting the number of polytopes to consider the shapes of polytopes, with the goal of delineating a more complete picture of neural networks.

Implicit bias of deep learning. A network used in practice is highly over-parameterized compared to the number of training samples. A natural question is often asked: why do deep networks not overfit? To address this question, extensive studies have proposed that a network is implicitly regularized to learn a simple solution. Implicit regularization is also referred to as an implicit bias. Gradient descent algorithms are widely believed to play an essential role in capacity control even when it is not specified in the loss function [Gunasekar et al., 2018, Soudry et al., 2018, Arora et al., 2019a, Sekhari et al., 2021, Lyu et al., 2021]. Du et al. [2018], Woodworth et al. [2020] showed that the optimization trajectory of neural networks stays close to the initialization with the help of neural tangent kernel theory. A line of works Arora et al. [2019b], Cao et al. [2019], Yang and Salman [2019], Choraria et al. [2022] have analyzed the bias of a deep network towards lower frequencies, which is referred to as the spectral bias. It was shown in Arora et al. [2018], Yu et al. [2017] that replacing weight matrices with low-rank matrices only deteriorates a network’s accuracy very moderately. Ongie and Willett [2022], Le and Jegelka identified the low-rank bias in linear layers of neural networks with gradient flow. Both theoretical derivation Tu et al. [2016], Li et al. [2020] and empirical findings Jing et al. [2020], Huh et al. [2021], Galanti et al. [2023] suggested that gradient descent tends to find a low-rank solution. What’s more, weight decay is a necessary condition to achieve the low-rank bias. In contrast, our investigation identifies a new implicit bias from the perspective of linear regions. Different from most implicit biases highlighting a certain property of a network, our implicit bias straightforwardly reveals what kind of simple functions a network learns. Our finding is relevant to the spectral bias. Since polytopes are both few and simple, a ReLU network does not produce a lot of oscillations in all directions, which roughly corresponds to a low-frequency solution.

3 Preliminaries

Throughout this paper, we always assume that the input space of an NN is a d -dimensional hypercube $C(d, B) := [-B, B]^d = \{\mathbf{x} = (x_1, x_2, \dots, x_d) \in \mathbb{R}^d : -B \leq x_i \leq B\}$ for some large enough constant B . Furthermore, we need the following definition for linear regions (polytopes).

Definition 1 (Linear regions (polytopes) Hanin and Rolnick [2019a]). *Suppose that \mathcal{N} is a ReLU NN with L hidden layers and input dimension d . An activation pattern of \mathcal{N} is a function \mathcal{P} from the set of neurons to the set $\{1, -1\}$, i.e., for each neuron z in \mathcal{N} , we have $\mathcal{P}(z) \in \{1, -1\}$. Let θ be a fixed set of parameters in \mathcal{N} , and \mathcal{P} be an activation pattern. Then the region corresponding to \mathcal{P} and θ is $\mathcal{R}(\mathcal{P}; \theta) := \{X \in C(d, B) : z(X; \theta) \cdot \mathcal{P}(z) > 0\}$, where $z(X; \theta)$ is the pre-activation of a neuron z in \mathcal{N} . A linear region of \mathcal{N} at θ is a non-empty set $\mathcal{R}(\mathcal{P}; \theta) \neq \emptyset$ for some activation pattern \mathcal{P} . Let $R_{\mathcal{N}, \theta}$ be the number of linear regions of \mathcal{N} at θ , i.e., $R_{\mathcal{N}, \theta} := \#\{\mathcal{R}(\mathcal{P}; \theta) : \mathcal{R}(\mathcal{P}; \theta) \neq \emptyset \text{ for some activation pattern } \mathcal{P}\}$. Moreover, let $R_{\mathcal{N}} := \max_{\theta} R_{\mathcal{N}, \theta}$ denote the maximum number of linear regions of \mathcal{N} when θ ranges over $\mathbb{R}^{\#\text{weights} + \#\text{bias}}$.*

In the following, Preliminary 1 shows that the polytopes created by a ReLU network are convex, which is the most important preliminary knowledge used in this manuscript. Since each polytope of a ReLU network is convex, as Figure 1 shows, one can further divide each polytope into simplices in a triangulation of polytopes to make it a simplicial complex (Preliminary 2), where a simplex is a fundamental unit. The number of simplices contained by a polytope can reflect the shape and complexity of the polytope. Then, Preliminary 3 introduces how to compute the vertices of polytopes. The detailed explanation of Preliminaries 1 and 3 can be seen in the Appendix.

Preliminary 1 (Polytopes of a neural network). *A neural network with ReLU activation partitions the input space into many polytopes (linear regions), such that the function represented by this neural network becomes linear when restricted in each polytope (linear region). Each polytope corresponds to a collection of activation states of all neurons, and each polytope is convex [Chu et al., 2018]. In this paper, we mainly focus on $(n_0 - 1)$ -dim faces of a n_0 -dim polytope. For convenience, we just simply use the terminology **face** to represent an $(n_0 - 1)$ -dim facet of an n_0 -dim polytope.*

Preliminary 2 (Simplex and simplicial complex). *A **simplex** is just a generalization of the notion of triangles or tetrahedrons to any dimensions. More precisely, a D -simplex S is a D -dimensional convex hull provided by convex combinations of $D + 1$ affinely independent vectors $\{\mathbf{v}_i\}_{i=0}^D \subset \mathbb{R}^D$.*

In other words, $S = \left\{ \sum_{i=0}^D \xi_i \mathbf{v}_i \mid \xi_i \geq 0, \sum_{i=0}^D \xi_i = 1 \right\}$. The convex hull of any subset of $\{\mathbf{v}_i\}_{i=0}^D$

*is called a face of S . A **simplicial complex** $\mathcal{S} = \bigcup_{\alpha} S_{\alpha}$ is composed of a set of simplices $\{S_{\alpha}\}$*

*satisfying: 1) every face of a simplex from \mathcal{S} is also in \mathcal{S} ; 2) the non-empty intersection of any two simplices $S_1, S_2 \in \mathcal{S}$ is a face of both S_1 and S_2 . A **triangulation of a polytope** P is a partition of P into simplices such that the union of all simplices equals P , and the intersection of any two simplices is a common face or empty. The triangulation of a polytope results in a simplicial complex.*

Preliminary 3 (Computing simplices in a polytope). *Given an L -hidden-layer ReLU network, neurons' activation states lead to a group of inequalities. A polytope with dimension n_0 is defined as $\{\mathbf{x} \in \mathbb{R}^{n_0} \mid \mathbf{a}_k \mathbf{x}^{\top} + b_k \leq 0, k \in [K]\}$, where $K = \sum_{i=1}^{L-1} n_i$ and n_i is the number of neurons in the i -th layer. Given these inequalities, the vertices of the polytope are derived based on the vertex enumeration algorithm [Avis and Fukuda, 1992]. Then, we can apply triangulation to these vertices to compute the number of simplices constituting this polytope.*

4 Deep ReLU Networks Have Simple Linear Regions

Here, by analyzing the number of simplices a polytope contains, we observe that linear regions formed by ReLU networks are surprisingly simple under both initialization and gradient descent. Although theoretically quite diverse linear regions can be derived, simple linear regions dominate, which is a high-capacity-low-reality phenomenon and a new implicit bias, which may explain why a deep learning model tends not to overfit. Combining the finding in [Hanin and Rolnick, 2019b], we can upgrade the conclusion to that deep ReLU networks have surprisingly *few* and *simple* linear regions. We validate our findings comprehensively and consistently at different initialization methods, network depths, sizes of the outer bounding box, biases, the bottleneck, network architecture, and input dimensions (Appendices H, I, J, and K). Furthermore, we showcase that during the training, although the number of linear regions increases, linear regions keep their simplicity. To ensure the preciseness of the discovery, our experiments are primarily on low-dimensional inputs.

4.1 Initialization

We validate four popular initialization methods: Xavier uniform, Xavier normal², Kaiming, orthogonal initialization [He et al., 2015]. For each initialization method, we use two different network architectures (3-40-20-1, 3-80-40-1). The bias values are set to 0.01 for all neurons. A total of 8,000 points are uniformly sampled from $[-1, 1]^3$ to compute the polytope. At the same time, we check the activation states of all neurons to avoid counting some polytopes more than once. Each run is repeated five times.

• **Initialization methods:** Figure 2 shows the histogram of the #simplices each polytope has under different initialization methods. Hereafter, if no special specification, the x-axis of all figures denotes the number of simplices a polytope has, and the y-axis denotes the count of polytopes with a certain number of simplices. Without loss of generality, suppose that in an experiment, the maximum number of simplices a polytope has is Ω , we deem a polytope with no more than $\Omega/3$ as simple. The spotlight is that for all initialization methods and network structures, simple polytopes significantly dominate over complicated polytopes. We calculate that simple polytopes take account for at least 57% and at most 76% of the total. In addition, among different initialization methods, the Xavier normal method tends to generate more uniform polytopes on four architectures. The achieved polytope is far simpler than the theoretically most complicated polytope.

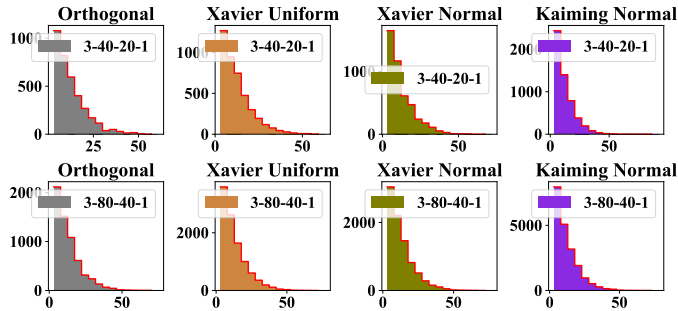


Figure 2: Deep ReLU networks have simple linear regions at different initialization methods.

• **Depths:** Here, we evaluate if the simplicity of polytopes still holds for deeper networks. This question is non-trivial, since a deeper network can theoretically generate more complicated polytopes. Will the depth break the simplicity? We choose four different widths (20, 40, 80, 160). For comprehensiveness, the network initialization methods are the Xavier uniform, Xavier normal, Kaiming, and orthogonal initialization. The depth is set to 5 and 8, respectively. The bias value is 0.01. Likewise, a total of 8,000 points are uniformly sampled from $[-1, 1]^3$ to compute the polytope. At the same time, we check the activation states of all neurons to avoid counting some polytopes more than once. Each run is repeated five times. The results under the Xavier uniform initialization are shown in Figure 3 (results under other initialization methods are put into the Appendix E), from which we draw three highlights. First, we find that both going deep and going wide can increase the number of polytopes at different initializations. But the effect of going deep is much more significant than that of going wide. Second, when the network goes deep, although the total number of polytopes increases, simple polytopes still dominate among all polytopes. Third, for different initialization methods and different depths, the dominating polytope is slightly different. For example, the dominating polytopes for the network 3-40-40-40-40-1 under Xavier normal initialization are those with 6~10 simplices, while the dominating polytopes for the network 3-20-20-20-20-1 under Xavier uniform initialization are those with 1~5 simplices.

• **Biases:** Here, we are curious about how the bias value of neurons will affect the distribution of polytopes. To address this issue, we set the bias values to 0, 0.01, 0.05, 0.1, respectively for the network 3-80-40-1. The outer bounding box is $[-1, 1]^3$. A total of 8,000 points are uniformly sampled from $[-1, 1]^3$ to compute the polytope. At the same time, we check the activation states of all neurons to avoid counting some polytopes more than once. Each run is repeated five times. The initialization methods are the Xavier uniform, Xavier normal, Kaiming, and orthogonal initialization. Figure 4 is from the Xavier uniform, and figures from other initialization methods are put into Appendix G. We observe that as the bias value increases, more polytopes are produced. However, the number of

²<https://pytorch.org/docs/stable/nn.init.html>

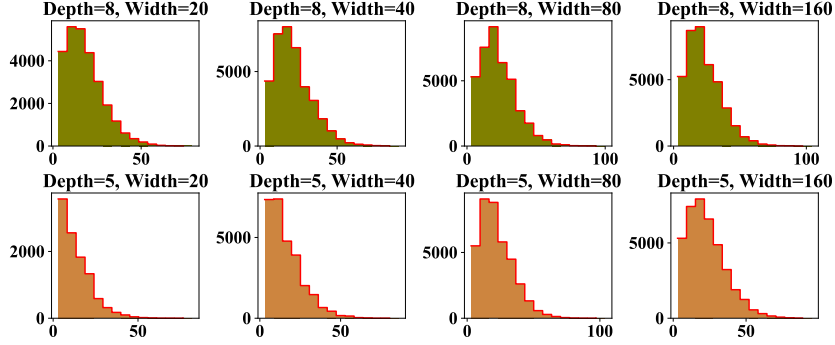


Figure 3: The simplicity holds true for deep networks under Xavier uniform initialization.

simple polytopes still takes up the majority. It is worthwhile mentioning that when the bias equals 0, the simplicity is crystal clear. The bias=0 is the extremal case, where all hyperplanes of the first layer intersect at the original point, and much fewer faces in polytopes are created.

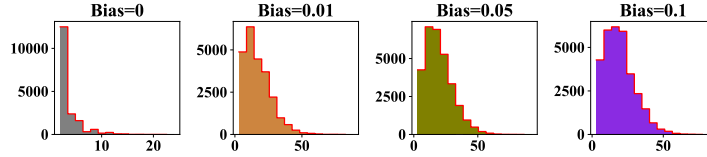


Figure 4: The simplicity holds true for different bias values under Xavier initialization.

4.2 Training

Earlier, we show that at the initialization stage, deep networks exhibit simple linear regions. It is natural to ask *will the simplicity of linear regions be broken during training?* We answer this question by training a fully-connected network using ReLU activation function on a real-world problem and counting the simplices of each polytope. The task is to predict if a COVID-19 patient will be at high risk, given one’s health status, living habits, and medical history. This prediction task has 388,878 raw samples, and each has 5 medical features including ‘HIPERTENSION’, ‘CARDIOVASCULAR’, ‘OBESITY’, ‘RENAL CHRONIC’, ‘TOBACCO’. The labels are ‘at risk’ or ‘no’. The detailed descriptions of data and this task can be referred to in Kaggle³. The data are preprocessed as follows: The discrete value is assigned to different attributes. If a patient has that pre-existing disease or habit, 1 will be assigned; otherwise, 0 will be assigned. Then, the data are randomly split into training and testing sets with a ratio of 0.8:0.2. We implement a network of 5-20-20-1. The optimizer is Adam with a learning rate of 0.1. The network is initialized by Xavier uniform. The loss function is the binary cross-entropy function. The epoch number is 400 to guarantee convergence. A total of 8,000 points are uniformly sampled from $[-1, 1]^3$ to compute the polytope. The outer bounding box is $[-5, 5]^3$ to ensure as many polytopes as possible are counted.

Figure 5 shows that as the training goes on, the total number of linear regions drops compared to the random initialization. Overall speaking, throughout the training, polytopes with no more than 1500 simplices take the majority. But the number of polytopes with 500-1000 simplices goes up, and the number of polytopes with fewer than 500 simplices goes down. It may suggest that the network may be primarily using them to fit data. Appendix L supplements results obtained from other initialization methods: Xavier normalization, Kaiming initialization, and orthogonal initialization.

We also train networks on MNIST, following the same procedure in [Hanin and Rolnick, 2019b]. Here, we can not compute the polytopes in 28×28 dimensional space because the vertex enumeration algorithm suffers the curse of dimensionality. Therefore, we visualize the polytopes in the cross-section plane. We initialize a network of size 784-7-7-6-10 with Kaiming normalization. The batch size is 128. The network is trained with Adam with a learning rate of 0.001. The total epoch number is set to 480, which ensures the convergence of the network.

³<https://www.kaggle.com/code/meirnazri/covid-19-risk-prediction>

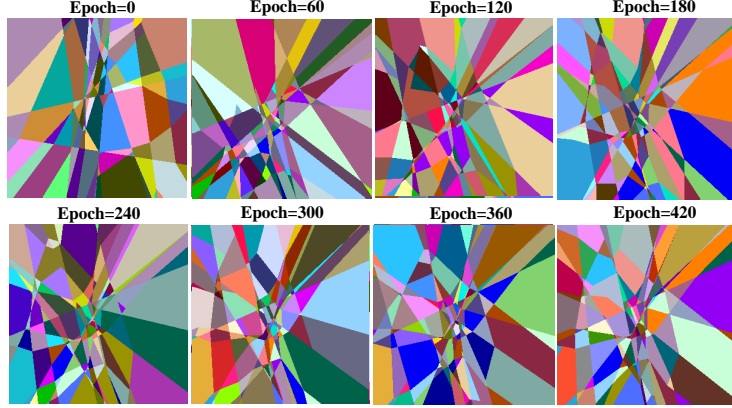


Figure 5: The results over a COVID dataset show that throughout the training, most polytopes are simple, despite that the number of linear regions drops during the training.

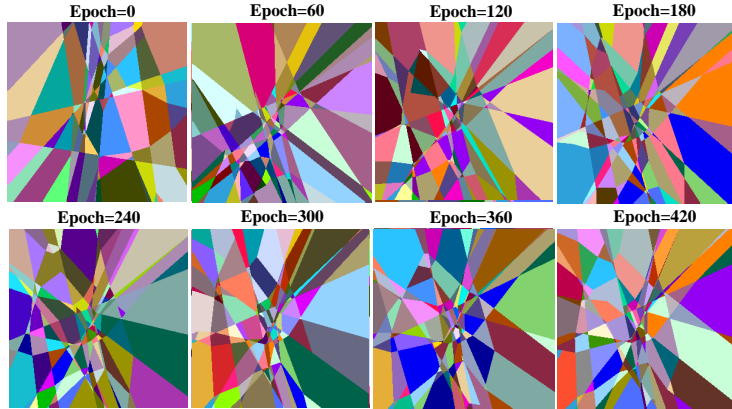


Figure 6: A cross-sectional visualization of the polytopes learned by a network over MNIST at different epochs. Almost all the polytopes are triangles or quadrilaterals.

Figure 6 shows the cross-section of the function learned by a network at different epochs. A cross-section is a plane that passes through two randomly-selected images from MNIST. Figure 6 shows that as the training goes on, the number of polytopes increases. But almost all the polytopes are triangles or quadrilaterals. Although these polytopes are from a cross-section other than the whole landscape, one can indirectly sense the simplicity of these polytopes.

5 Theoretical Explanation (Simple Polytope Theorem)

In this section, we seek to provide a theoretical explanation for the simple polytope phenomenon. We establish a theorem that bounds the average face numbers of polytopes of a network to a small number under some mild assumption, thereby substantiating our finding. Our theoretical derivation is twofold: initialization and after training.

Geometric heuristics of multi-layer networks. Generically, we argue that a deep ReLU network should still have simple polytopes. We think that the simplicity of polytopes is given rise to two reasons. (1) First, since a ReLU network divides the space into many local polytopes, to yield a complicated polytope from a local polytope, two or more hyperplanes associated with neurons in the later layers should intersect within the given local polytope, which is hard because the area of polytopes is typically small. In [Hanin and Rolnick, 2019b], where a deep ReLU network was proved to have few polytopes because hyperplanes do not cross in a local polytope. Without crossing, complicated polytopes will not emerge either. As such, the complexity of polytopes probably only increases moderately as the network goes deeper. (2) Take a polytope P with k faces as an example. If we add one hyperplane to divide P into two new polytopes P_1 and P_2 , then the total number of faces increases by $k_0 + 2$ (the hyperplane itself should be counted twice), if the hyperplane intersects with k_0 faces in P . Usually, k_0 should be smaller than k because a hyperplane cannot cross all faces of P , thus the average number of edges of P_1 and P_2 becomes $(k + k_0 + 2)/2 \leq k$. By this idea, we can see that in most cases, the number of the average number of faces in polytopes of a general

multi-layer ReLU neural network \mathcal{N} will not increase when the number of layers gets deeper, since adding the hyperplanes one by one in a polytope will not increase the average number of faces in the new polytopes they divide.

5.1 Initialization

Theorem 1 (Simple Polytope Theorem, One-hidden-layer NNs). *Let \mathcal{N} be a one-hidden-layer fully-connected ReLU NN with d inputs and n hidden neurons, where d is a fixed positive integer. Suppose that n hyperplanes generated by n hidden neurons are in general position. Let $C(d, B) := [-B, B]^d$ be the input space of \mathcal{N} . Furthermore, assume that n and B are large enough, then the average number of faces in linear regions of \mathcal{N} is at most $2d + 1$.*

Theorem 2 (Simple Polytope Theorem, Multi-layer NNs, $d = 2$). *Let \mathcal{N} be an L -layer fully-connected ReLU NN with $d = 2$ inputs and n_i hidden neurons in the i -th hidden layer. Let $C(d, B) := [-B, B]^d$ be the input space of \mathcal{N} . Furthermore, assume that n_i and B are large enough, then the average number of faces in linear regions of \mathcal{N} is at most $2d = 4$.*

Theorem 3 (Simple Polytope Theorem, Multi-layer NNs with Zero Biases). *Let \mathcal{N} be an L -layer fully-connected ReLU NN with d inputs and n_i hidden neurons in the i -th hidden layer where d is a fixed positive integer. Suppose that all the biases of \mathcal{N} are equal to zero. Let $C(d, B) := [-B, B]^d$ be the input space of \mathcal{N} . Furthermore, assume that the number of hidden neurons and B are large enough, then the average number of faces in linear regions of \mathcal{N} is at most $3d - 1$.*

Proof. Please see Appendix B. □

Interpretation of these bounds. It is desirable that no matter how deep a network is, the average number of faces of polytopes produced by a network is only concerned with the input dimension. We highlight that this bound is an intrinsic quantity regarding a network. Considering that $3d - 1$ is a rather small bound, it can justify why simple polytopes dominate. If the dominating polytopes are complex polytopes, the average face number should surpass $3d - 1$ a lot. If simple polytopes only take up a small portion, the average face number will be larger than $3d - 1$, too. Although we assume that the network is wide in deriving the bound, based on our geometric heuristics, the average face number should also be small for narrow networks. We leave this question for future exploration.

Theorem 3 and Theorems 1, 2 are built for cases of zero biases and non-zero biases, respectively. It is a general practice to initialize biases with 0 before training a network, *e.g.*, biases are often set to 0 in Xavier initialization Glorot and Bengio [2010]. Therefore, Theorem 3 aligns with reality well. In addition, a ReLU network with zero biases becomes homogeneous, *i.e.*, $\mathcal{N}(\alpha\theta; \cdot) = \alpha^L \mathcal{N}(\theta; \cdot)$, which is a widely-used setting when investigating implicit bias Lyu and Li [2020], Vardi et al. [2022]. Non-zero biases are so complicated to give a general and complete theorem for arbitrary cases. We only make success for one-hidden-layer networks with an arbitrary dimension and multi-layer networks with $d = 2$.

Deriving Theorems 1 and 3 is tricky. The basic idea can be divided into two parts: Firstly, we derive the upper bound of simplices depending on the observation that for each $(d - 1)$ -dim face of a d -dim polytope, it can only be a face for one unique simplex in a triangulation of this polytope, thus the total number of simplices in triangulations of polytopes must be smaller than or equal to the total number of $(d - 1)$ -dim faces in all polytopes. Therefore, we just need to derive the upper bound for the total number of $(d - 1)$ -dim faces in all polytopes generated by a neural network \mathcal{N} , which can be done by induction on the number of layers of \mathcal{N} . Secondly, we derive the number of polytopes by the techniques and results from the classic hyperplane arrangement theories (see Stanley et al. [2004]). Finally, the quotient between the upper bound of simplices and the number of polytopes gives the upper bound for the average number of faces in linear regions of \mathcal{N} .

5.2 After Training: Low-Rank

Can we theoretically derive that polytopes remain simple after training? It was shown that gradient descent-based optimization learns weight matrices of low rank Galanti et al. [2023], Huh et al. [2021]. Therefore, under the low-rank setting, We also investigate if the polytopes are simple after the training. We derive Theorems 4 and 5 to substantiate that after training, polytopes remain simple.

Theorem 4 (Simple Polytope Theorem, Multi-Layer NNs with Zero Biases and Low-rank Weight Matrices). *Let \mathcal{N} be an L -layer fully-connected ReLU NN with d inputs and n_i hidden neurons in the i -th hidden layer where d is a fixed positive integer. Assume that the weight matrix $W \in \mathbb{R}^{d \times n}$ has*

rank $d_0 \leq d$. Suppose that all the biases of \mathcal{N} are equal to zero. Let $C(d, B) := [-B, B]^d$ be the input space of \mathcal{N} . Furthermore, assume that the number of hidden neurons and B are large enough, then the average number of faces in linear regions of \mathcal{N} is at most $2d_0 + d - 1$.

Theorem 5 (Simple Polytope Theorem, One-hidden-layer NNs, Low-rank Weight Matrices). *Let \mathcal{N} be a one-hidden-layer fully-connected ReLU NN with d inputs and n hidden neurons, where d is a fixed positive integer. Assume that the weight matrix $W \in \mathbb{R}^{d \times n}$ has rank $d_0 \leq d$. Suppose that any d_0 hyperplanes generated by any d_0 hidden neurons are in general position. Let $C(d, B) := [-B, B]^d$ be the input space of \mathcal{N} . Furthermore, assume that n and B are large enough, then the average number of faces in linear regions of \mathcal{N} is at most $2d_0 + 1$.*

Proof. For proofs of Theorems 4 and 5, please see Appendix B. □

According to Theorems 4 and 5, we can see that when the weight matrix has a lower rank d_0 , which is smaller than the input dimension d , then the average number of faces in linear regions of \mathcal{N} is determined by d_0 and irrelevant to the input dimension d . This means that, after the training of a ReLU neural network, if the weight matrices become low-rank matrices (which is suggested by Galanti et al. [2023], Huh et al. [2021]), then the average number of faces in linear regions of \mathcal{N} would be much smaller, which means that the linear regions tend to be much simpler after training.

6 Discussion

Estimating the shape of polytopes by Monte Carlo sampling. *How to empirically estimate the shape of polytopes for high-dimensional inputs?* Our theoretical derivation suggests that one can use the number of faces of a polytope as a proxy for #simplices to describe the shape of polytopes. Thus, we don't need to compute the vertices and triangulation that are time-consuming for high-dimensional space. Since a polytope with the dimension n_0 is defined as $\{\mathbf{x} \in \mathbb{R}^{n_0} \mid \mathbf{a}_k \mathbf{x}^\top + b_k \leq 0, k \in [K]\}$, computing the number of faces is equivalent to finding which inequalities are non-redundant. Non-redundant inequalities are the faces of a polytope. Determining the non-redundant inequalities can be done by the hit-and-run algorithms, a representative Monte Carlo sampling method. Appendix M shows the methodology and provides an example that estimates the number of faces of polytopes formed by a variant of LeNet-5 architectures for 784 dimensions.

Extension to CNNs. Our results on the average number of faces in polytopes generated by multi-layer ReLU NNs can be extended to many kinds of architectures such as CNNs. Theoretically, both CNNs and fully-connected networks conform to the geometric restrictions. Since one hyperplane cannot cross all faces of a polytope, the average face number will not tend to increase. In Appendix M, using Monte Carlo estimation, experiments on a LeNet-5 variant discovered that the average number of faces polytopes have is much smaller than the maximum number of inequalities, suggesting that simple polytopes are also held by CNNs.

#Simplices as a leverage for other problems. The focus of this draft is to use #simplices to study the shape of polytopes formed by a ReLU network. However, since #simplices that concerns the shape of polytopes is a more fine-grained characterization compared to #polytopes, one can also use #simplices as a complexity measure to describe the expressivity of a ReLU network. Appendix C lists the potential advantages of #simplices as a complexity measure over #polytopes in terms of uniqueness via modularization and applicability to classification networks. As a basic complexity measure, #simplices can help us understand the behavior of a network from a different angle such as explaining the power of popular shortcut networks such as ResNet and analyzing the impact of regularization on a network's space partition.

For example, 1) in Appendix D, Theorems 6 and 7 summarize the upper and lower bounds of the maximum #simplices of a feedforward ReLU network and ResNet. It is found that the upper bound of the maximum #simplices of a feedforward ReLU network and ResNet are the same. In other words, the addition of residual connections may not increase the expressivity of a network a lot. The main advantage of residual connections lies in the optimization because they can facilitate the flow of gradients. 2) In Appendix N, we use the #simplices to investigate the impact of weight decay on the shapes of learned polytopes. It is observed that as the weight decay is exerted more and more heavily, the number of polytopes goes down and on the other hand, learned polytopes have fewer simplices, which means they are simpler.

7 Conclusion and Limitation

In this manuscript, we have advocated studying the properties of polytopes instead of just counting them, towards revealing other valuable properties of a neural network. Then, we observed that deep ReLU networks have simple linear regions, which is not only a fundamental characterization but also an implicit bias for ReLU networks explaining why deep networks do not overfit. Lastly, we have mathematically established a small bound for the average number of faces in polytopes, therefore supplying an explanation for the simple polytope phenomenon.

An important limitation of our work is that we don't fully illustrate the relationship between our implicit bias and others. Just like in mathematics, there can be more than one set of axioms for an axiom system, and different axiom systems can be mutually deduced. Since the implicit bias is derived from gradient descent, different implicit biases should be related to one another. An important future direction will be building the relationship between different forms of implicit biases Galanti et al. [2023]. If so, the understanding of implicit biases can be greatly deepened.

References

- Raman Arora, Amitabh Basu, Poorya Mianjy, and Anirbit Mukherjee. Understanding deep neural networks with rectified linear units. *arXiv preprint arXiv:1611.01491*, 2016.
- Sanjeev Arora, Rong Ge, Behnam Neyshabur, and Yi Zhang. Stronger generalization bounds for deep nets via a compression approach. In *International Conference on Machine Learning*, pages 254–263. PMLR, 2018.
- Sanjeev Arora, Nadav Cohen, Wei Hu, and Yuping Luo. Implicit regularization in deep matrix factorization. *Advances in Neural Information Processing Systems*, 32, 2019a.
- Sanjeev Arora, Simon Du, Wei Hu, Zhiyuan Li, and Ruosong Wang. Fine-grained analysis of optimization and generalization for overparameterized two-layer neural networks. In *International Conference on Machine Learning*, pages 322–332. PMLR, 2019b.
- David Avis and Komei Fukuda. A pivoting algorithm for convex hulls and vertex enumeration of arrangements and polyhedra. *Discrete & Computational Geometry*, 8(3):295–313, 1992.
- Randall Balestriero and Richard G Baraniuk. Mad max: Affine spline insights into deep learning. *Proceedings of the IEEE*, 109(5):704–727, 2020.
- HCP Berbee, CGE Boender, AHG Rinnooy Ran, CL Scheffer, Robert L Smith, and Jan Telgen. Hit-and-run algorithms for the identification of nonredundant linear inequalities. *Mathematical Programming*, 37:184–207, 1987.
- Monica Bianchini and Franco Scarselli. On the complexity of neural network classifiers: A comparison between shallow and deep architectures. *IEEE transactions on neural networks and learning systems*, 25(8):1553–1565, 2014.
- Yuan Cao, Zhiying Fang, Yue Wu, Ding-Xuan Zhou, and Quanquan Gu. Towards understanding the spectral bias of deep learning. *arXiv preprint arXiv:1912.01198*, 2019.
- Richard J Caron, Arnon Boneh, and Shahar Boneh. Redundancy. *Advances in Sensitivity Analysis and Parametric Programming*, pages 449–489, 1997.
- Wuyang Chen, Xinyu Gong, and Zhangyang Wang. Neural architecture search on imagenet in four gpu hours: A theoretically inspired perspective. *arXiv preprint arXiv:2102.11535*, 2021.
- Moulik Choraria, Leello Tadesse Dadi, Grigorios Chrysos, Julien Mairal, and Volkan Cevher. The spectral bias of polynomial neural networks. *arXiv preprint arXiv:2202.13473*, 2022.
- Lingyang Chu, Xia Hu, Juhua Hu, Lanjun Wang, and Jian Pei. Exact and consistent interpretation for piecewise linear neural networks: A closed form solution. In *Proceedings of the 24th ACM SIGKDD International Conference on Knowledge Discovery & Data Mining*, pages 1244–1253, 2018.

- Nadav Cohen, Or Sharir, and Amnon Shashua. On the expressive power of deep learning: A tensor analysis. In *Conference on learning theory*, pages 698–728. PMLR, 2016.
- Francesco Croce, Maksym Andriushchenko, and Matthias Hein. Provable robustness of relu networks via maximization of linear regions. In *the 22nd International Conference on Artificial Intelligence and Statistics*, pages 2057–2066. PMLR, 2019.
- Simon S Du, Xiyu Zhai, Barnabas Poczos, and Aarti Singh. Gradient descent provably optimizes over-parameterized neural networks. *arXiv preprint arXiv:1810.02054*, 2018.
- Feng-Lei Fan, Rongjie Lai, and Ge Wang. Quasi-equivalence of width and depth of neural networks. *arXiv preprint arXiv:2002.02515*, 2020.
- Tomer Galanti, Zachary Siegel, Aparna Gupte, and Tomaso Poggio. Sgd and weight decay provably induce a low-rank bias in deep neural networks. Technical report, Center for Brains, Minds and Machines (CBMM), 2023.
- Matteo Gamba, Stefan Carlsson, Hossein Azizpour, and Mårten Björkman. Hyperplane arrangements of trained convnets are biased. *arXiv preprint arXiv:2003.07797*, 2020.
- Xavier Glorot and Yoshua Bengio. Understanding the difficulty of training deep feedforward neural networks. In *Proceedings of the thirteenth international conference on artificial intelligence and statistics*, pages 249–256. JMLR Workshop and Conference Proceedings, 2010.
- Suriya Gunasekar, Jason Lee, Daniel Soudry, and Nathan Srebro. Characterizing implicit bias in terms of optimization geometry. In *International Conference on Machine Learning*, pages 1832–1841. PMLR, 2018.
- Boris Hanin and David Rolnick. Complexity of linear regions in deep networks. In *International Conference on Machine Learning*, pages 2596–2604, 2019a.
- Boris Hanin and David Rolnick. Deep relu networks have surprisingly few activation patterns. In *Advances in Neural Information Processing Systems*, pages 359–368, 2019b.
- Kaiming He, Xiangyu Zhang, Shaoqing Ren, and Jian Sun. Delving deep into rectifiers: Surpassing human-level performance on imagenet classification. In *IEEE International Conference on Computer Vision*, pages 1026–1034, 2015.
- Kaiming He, Xiangyu Zhang, Shaoqing Ren, and Jian Sun. Deep residual learning for image recognition. In *Proceedings of the IEEE conference on computer vision and pattern recognition*, pages 770–778, 2016.
- Qiang Hu and Hao Zhang. Nearly-tight bounds on linear regions of piecewise linear neural networks. *arXiv preprint arXiv:1810.13192*, 2018.
- Xia Hu, Weiqing Liu, Jiang Bian, and Jian Pei. Measuring model complexity of neural networks with curve activation functions. In *Proceedings of the 26th ACM SIGKDD International Conference on Knowledge Discovery & Data Mining*, pages 1521–1531, 2020.
- Xia Hu, Lingyang Chu, Jian Pei, Weiqing Liu, and Jiang Bian. Model complexity of deep learning: A survey. *Knowledge and Information Systems*, 63(10):2585–2619, 2021.
- Minyoung Huh, Hossein Mobahi, Richard Zhang, Brian Cheung, Pulkit Agrawal, and Phillip Isola. The low-rank simplicity bias in deep networks. *arXiv preprint arXiv:2103.10427*, 2021.
- Li Jing, Jure Zbontar, et al. Implicit rank-minimizing autoencoder. *Advances in Neural Information Processing Systems*, 33:14736–14746, 2020.
- Thien Le and Stefanie Jegelka. Training invariances and the low-rank phenomenon: beyond linear networks. In *International Conference on Learning Representations*.
- Zhiyuan Li, Yuping Luo, and Kaifeng Lyu. Towards resolving the implicit bias of gradient descent for matrix factorization: Greedy low-rank learning. *arXiv preprint arXiv:2012.09839*, 2020.

- Kaifeng Lyu and Jian Li. Gradient descent maximizes the margin of homogeneous neural networks. In *International Conference on Learning Representations*, 2020.
- Kaifeng Lyu, Zhiyuan Li, Runzhe Wang, and Sanjeev Arora. Gradient descent on two-layer nets: Margin maximization and simplicity bias. *Advances in Neural Information Processing Systems*, 34:12978–12991, 2021.
- Mehryar Mohri, Afshin Rostamizadeh, and Ameet Talwalkar. *Foundations of machine learning*. MIT press, 2018.
- Guido Montúfar. Notes on the number of linear regions of deep neural networks. *Sampling Theory Appl., Tallinn, Estonia, Tech. Rep.*, 2017.
- Guido F Montufar, Razvan Pascanu, Kyunghyun Cho, and Yoshua Bengio. On the number of linear regions of deep neural networks. In *Advances in neural information processing systems*, pages 2924–2932, 2014.
- Greg Ongie and Rebecca Willett. The role of linear layers in nonlinear interpolating networks. *arXiv preprint arXiv:2202.00856*, 2022.
- Yookoon Park, Sangho Lee, Gunhee Kim, and David Blei. Unsupervised representation learning via neural activation coding. In *International Conference on Machine Learning*, pages 8391–8400. PMLR, 2021.
- Razvan Pascanu, Guido Montufar, and Yoshua Bengio. On the number of response regions of deep feed forward networks with piece-wise linear activations. *arXiv preprint arXiv:1312.6098*, 2013.
- Ben Poole, Subhaneil Lahiri, Maithra Raghu, Jascha Sohl-Dickstein, and Surya Ganguli. Exponential expressivity in deep neural networks through transient chaos. *Advances in neural information processing systems*, 29, 2016.
- Stefan Schonsheck, Jie Chen, and Rongjie Lai. Chart auto-encoders for manifold structured data. *arXiv preprint arXiv:1912.10094*, 2019.
- Ayush Sekhari, Karthik Sridharan, and Satyen Kale. Sgd: The role of implicit regularization, batch-size and multiple-epochs. *Advances In Neural Information Processing Systems*, 34:27422–27433, 2021.
- Thiago Serra, Christian Tjandraatmadja, and Srikumar Ramalingam. Bounding and counting linear regions of deep neural networks. In *International Conference on Machine Learning*, pages 4558–4566. PMLR, 2018.
- Daniel Soudry, Elad Hoffer, Mor Shpigel Nacson, Suriya Gunasekar, and Nathan Srebro. The implicit bias of gradient descent on separable data. *The Journal of Machine Learning Research*, 19(1): 2822–2878, 2018.
- Richard P. Stanley. An introduction to hyperplane arrangements. In *Lecture Notes, IAS/Park City Mathematics Institute*, 2004.
- Richard P Stanley et al. An introduction to hyperplane arrangements. *Geometric combinatorics*, 13 (389-496):24, 2004.
- Matus Telgarsky. Representation benefits of deep feedforward networks. *arXiv preprint arXiv:1509.08101*, 2015.
- Csaba D Toth, Joseph O’Rourke, and Jacob E Goodman. *Handbook of discrete and computational geometry*. CRC press, 2017.
- Stephen Tu, Ross Boczar, Max Simchowitz, Mahdi Soltanolkotabi, and Ben Recht. Low-rank solutions of linear matrix equations via procrustes flow. In *International Conference on Machine Learning*, pages 964–973. PMLR, 2016.
- Gal Vardi, Gilad Yehudai, and Ohad Shamir. Gradient methods provably converge to non-robust networks. In *Advances in Neural Information Processing Systems*, 2022.

- Blake Woodworth, Suriya Gunasekar, Jason D Lee, Edward Moroshko, Pedro Savarese, Itay Golan, Daniel Soudry, and Nathan Srebro. Kernel and rich regimes in overparametrized models. In *Conference on Learning Theory*, pages 3635–3673. PMLR, 2020.
- Huan Xiong, Lei Huang, Mengyang Yu, Li Liu, Fan Zhu, and Ling Shao. On the number of linear regions of convolutional neural networks. In *International Conference on Machine Learning*, pages 10514–10523. PMLR, 2020.
- Greg Yang and Hadi Salman. A fine-grained spectral perspective on neural networks. *arXiv preprint arXiv:1907.10599*, 2019.
- Xiyu Yu, Tongliang Liu, Xinchao Wang, and Dacheng Tao. On compressing deep models by low rank and sparse decomposition. In *Proceedings of the IEEE conference on computer vision and pattern recognition*, pages 7370–7379, 2017.
- T. Zaslavsky. *Facing up to arrangements : face-count formulas for partitions of space by hyperplanes*. Number 154 in *Memoirs of the American Mathematical Society*. American Mathematical Society, 1975.
- T Zaslavsky. Facing up to arrangements: face-count formulas for partitions of space by hyperplanes. *Memoirs of American Mathematical Society*, 154:1–95, 1997.
- Xiao Zhang and Dongrui Wu. Empirical studies on the properties of linear regions in deep neural networks. *arXiv preprint arXiv:2001.01072*, 2020.

Contents of Appendices

Section A introduces why ReLU networks partition the space into polytopes and how to compute the simplices that constitute each polytope.

Section B theoretically estimates the average number of faces in linear regions of neural networks under initialization and after training.

Section C introduces the potential of #simplices as a complexity measure.

Section D estimate the upper and lower bounds of the maximum #simplices of different networks such as feedforward networks and networks with residual connections.

Section E provides supplementary experimental results for networks with different depths.

Section F provides supplementary experimental results for much deeper networks (depth=34 and 50).

Section G provides supplementary experimental results for networks initialized with different biases.

Section H provides supplementary experimental results for bounding boxes of different sizes.

Section I provides supplementary experiments for different network structures such as pyramidal and inverted pyramidal structures.

Section J provides supplementary experiment results for networks with bottleneck layers.

Section K supplements more experimental results for different dimensions.

Section L provides supplementary results on the COVID Dataset under other initializations.

Section M shows that we can estimate the number of faces of polytopes by monte carlo sampling.

Section N shows that we can use the number of simplices to investigate how different regularization strategies can impact the shape of polytopes.

A Simplicies, Polytopes, and Their Computation

A.1 Notations of a Network

For convenience and consistency, we inherit notations from [Chu et al., 2018]. For a ReLU network that contains L hidden layers, we write the l -th layer as \mathcal{L}_l . Specially, \mathcal{L}_0 is the input layer, \mathcal{L}_{L+1} is the output layer, and the other layers $\mathcal{L}_l, l \in \{1, 2, \dots, L\}$ are hidden layers. Hidden layers' neurons are called hidden neurons. Let n_l represent the number of neurons in \mathcal{L}_l .

Given the i -th neuron of the l -th hidden layer, we denote by $\mathbf{b}_i^{(l)}$ its bias, by $\mathbf{a}_i^{(l)}$ its output, and by $\mathbf{z}_i^{(l)}$ the total weighted sum of its inputs plus the bias. For all the n_l neurons in \mathcal{L}_l , we arrange all their biases into a vector $\mathbf{b}^{(l)} = [\mathbf{b}_1^{(l)}, \dots, \mathbf{b}_{n_l}^{(l)}]^\top$, their outputs into a vector $\mathbf{a}^{(l)} = [\mathbf{a}_1^{(l)}, \dots, \mathbf{a}_{n_l}^{(l)}]^\top$, and their inputs into a vector $\mathbf{z}^{(l)} = [\mathbf{z}_1^{(l)}, \dots, \mathbf{z}_{n_l}^{(l)}]^\top$. Neurons in two neighbor layers are linked by weighted edges. Denote by $W_{ij}^{(l)}$ the weight of the edge between the i -th neuron in \mathcal{L}_{l+1} and the j -th neuron in \mathcal{L}_l . For $l \in \{1, \dots, L\}$, we compute $\mathbf{z}^{(l+1)}$ by

$$\mathbf{z}^{(l+1)} = W^{(l)} \mathbf{a}^{(l)} + \mathbf{b}^{(l)}, \quad (1)$$

where $W^{(l)}$ is an n_{l+1} -by- n_l matrix.

Let $\sigma : \mathbb{R} \rightarrow \mathbb{R}$ be the ReLU activation function. We have $\mathbf{a}_i^{(l)} = \sigma(\mathbf{z}_i^{(l)})$ for all $l \in \{1, \dots, L\}$. In an element-wise fashion, we write $\sigma(\mathbf{z}^{(l)}) = [\sigma(\mathbf{z}_1^{(l)}), \dots, \sigma(\mathbf{z}_{n_l}^{(l)})]^\top$. Then, for $l \in \{1, \dots, L\}$, we have

$$\mathbf{a}^{(l)} = \sigma(\mathbf{z}^{(l)}). \quad (2)$$

The input is $\mathbf{x} \in \mathcal{X}$, where $\mathcal{X} \in \mathbb{R}^d$, and \mathbf{x}_i is the i -th dimension of \mathbf{x} . The input layer \mathcal{L}_0 contains $n_0 = d$ nodes, where $\mathbf{a}_i^{(0)} = \mathbf{x}_i, i \in \{1, \dots, d\}$. The output of the network is $\mathbf{a}^{(L+1)} \in \mathcal{Y}$, where $\mathcal{Y} \subseteq \mathbb{R}^{n_{L+1}}$. The output layer \mathcal{L}_{L+1} employs the softmax function: $\mathbf{a}^{(L+1)} = \text{softmax}(\mathbf{z}^{(L+1)})$.

A.2 Deriving Polytopes of a Network

For the i -th hidden neuron in \mathcal{L}_l , $\sigma(\mathbf{z}_i^{(l)})$ is in the following form:

$$\sigma(\mathbf{z}_i^{(l)}) = \begin{cases} \mathbf{z}_i^{(l)}, & \text{if } \mathbf{z}_i^{(l)} \geq 0 \\ 0, & \text{if } \mathbf{z}_i^{(l)} < 0, \end{cases} \quad (3)$$

where $\sigma(\mathbf{z}_i^{(l)})$ consists of two linear parts. Given a network, an instance $\mathbf{x} \in \mathcal{X}$ determines the value of $\mathbf{z}_i^{(l)}$, and further determines $\sigma(\mathbf{z}_i^{(l)}) = 0$ or $\sigma(\mathbf{z}_i^{(l)}) = \mathbf{z}_i^{(l)}$. According to which part $\sigma(\mathbf{z}_i^{(l)})$ falls into, one can encode the activation status of each hidden neuron by two states, each of which uniquely corresponds to one part of $\sigma(\mathbf{z}_i^{(l)})$. Denote by $\mathbf{c}_i^{(l)} \in \{1, 0\}$ the state of the i -th hidden neuron in \mathcal{L}_l , we have $\mathbf{z}_i^{(l)} \geq 0$ if and only if $\mathbf{c}_i^{(l)} = 1$ and $\mathbf{z}_i^{(l)} < 0$ if and only if $\mathbf{c}_i^{(l)} = 0$. The states of different hidden neurons usually differ from each other.

Let $\mathbf{c}^{(l)} = [\mathbf{c}_1^{(l)}, \dots, \mathbf{c}_{n_l}^{(l)}]$ be the states of all hidden neurons in \mathcal{L}_l and $\mathbf{C} = [\mathbf{c}^{(1)}, \dots, \mathbf{c}^{(L)}]$ specify the collective states of all hidden neurons. \mathbf{C} of a given fixed network is uniquely determined by the instance \mathbf{x} . We write the function that maps an instance $\mathbf{x} \in \mathcal{X}$ to a configuration $\mathbf{C} \in \{1, 0\}^N$ as $\text{conf} : \mathcal{X} \rightarrow \{1, 0\}^N$, where $N = \sum_{i=0}^{L-1} n_i$. Then, we rewrite Eq. (2) as

$$\mathbf{a}^{(l)} = \sigma(\mathbf{z}^{(l)}) = \mathbf{c}^{(l)} \circ \mathbf{z}^{(l)}, \quad (4)$$

where $\mathbf{c}^{(l)} \circ \mathbf{z}^{(l)}$ is the Hadamard product between $\mathbf{c}^{(l)}$ and $\mathbf{z}^{(l)}$.

By plugging $\mathbf{a}^{(l)}$ into Eq. (1), we rewrite $\mathbf{z}^{(l+1)}$ as

$$\mathbf{z}^{(l+1)} = W^{(l)} \left(\mathbf{c}^{(l)} \circ \mathbf{z}^{(l)} \right) + \mathbf{b}^{(l)} = \tilde{W}^{(l)} \mathbf{z}^{(l)} + \tilde{\mathbf{b}}^{(l)}, \quad (5)$$

where $\tilde{\mathbf{b}}^{(l)} = \mathbf{b}^{(l)}$, and $\tilde{W}^{(l)} = W^{(l)} \circ \mathbf{c}^{(l)}$ is the generalized Hadamard product, such that the entry at the i -th row and j -th column of $\tilde{W}^{(l)}$ is $\tilde{W}_{ij}^{(l)} = W_{ij}^{(l)} \mathbf{c}_j^{(l)}$.

By iteratively enforcing Eq. (5), we can write $\mathbf{z}^{(l+1)}$, $l \in \{1, \dots, L\}$ as

$$\mathbf{z}^{(l+1)} = \left(\prod_{k=1}^l \tilde{W}^{(k)} \right) \mathbf{z}^{(1)} + \sum_{h=1}^l \left(\prod_{k=h+1}^l \tilde{W}^{(k)} \right) \tilde{\mathbf{b}}^{(h)}. \quad (6)$$

Substituting $\mathbf{z}^{(1)} = W^{(0)} \mathbf{x} + \mathbf{b}^{(1)}$ into the above equation, we rewrite $\mathbf{z}^{(l+1)}$, $l \in \{1, \dots, L\}$ as

$$\begin{aligned} & \mathbf{z}^{(l+1)} \\ &= \left(\prod_{k=1}^l \tilde{W}^{(k)} \right) (W^{(0)} \mathbf{x} + \mathbf{b}^{(1)}) + \sum_{h=1}^l \left(\prod_{k=h+1}^l \tilde{W}^{(k)} \right) \tilde{\mathbf{b}}^{(h)} \\ &= \left(\prod_{k=0}^l \tilde{W}^{(k)} \right) \mathbf{x} + \mathbf{b}^{(1)} \left(\prod_{k=1}^l \tilde{W}^{(k)} \right) + \sum_{h=1}^l \left(\prod_{k=h+1}^l \tilde{W}^{(k)} \right) \tilde{\mathbf{b}}^{(h)} \\ &= \hat{W}^{(0:l)} \mathbf{x} + \hat{\mathbf{b}}^{(0:l)}, \end{aligned} \quad (7)$$

where $\hat{W}^{(0:l)}$ is the coefficient matrix of \mathbf{x} , and $\hat{\mathbf{b}}^{(0:l)}$ is the sum of the remaining bias terms. Naturally, $F(\mathbf{x})$ is

$$F(\mathbf{x}) = \text{softmax} \left(\hat{W}^{(0:L)} \mathbf{x} + \hat{\mathbf{b}}^{(0:L)} \right). \quad (8)$$

For a fixed network and a fixed instance \mathbf{x} , $\hat{W}^{(0:l)}$ and $\hat{\mathbf{b}}^{(0:l)}$ are constant parameters uniquely determined by activation states of all neurons: $\mathbf{C} = \text{conf}(\mathbf{x})$. Furthermore, according to Eq. (3), \mathbf{C} leads to a group of inequalities:

$$(2\mathbf{c}^{(l+1)} - 1) \circ (\hat{W}^{(0:l)} \mathbf{x} + \hat{\mathbf{b}}^{(0:l)}) \geq 0, \quad l = 0, \dots, L-1, \quad (9)$$

which encompasses a convex polytope according to the H -definition of polytopes (Chapter 16, Toth et al. [2017]). If $\text{conf}(\mathbf{x}_1) = \text{conf}(\mathbf{x}_2)$, \mathbf{x}_1 and \mathbf{x}_2 lie in the same polytope due to the uniqueness.

A.3 Computing #Simplices and Polytopes with Vertex Enumeration Algorithm

Algorithm 1 Calculate the #simplex of a polytope of a neural network

- 1: Identify a collective activation state of all neurons
 - 2: Derive a group of inequalities whose hyperplanes encompass the targeted polytope
 - 3: Vertex enumeration algorithm to derive the vertices of the polytope
 - 4: Delaunay triangulation
 - 5: Count #simplices
-

Next, what is essential is to numerically compute #simplices. Unfortunately, the exact computation relies on enumerating all collective states of neurons, which is only possible i) when the total number of neurons in a network is small or ii) when the input dimension is low. For the former, we can enumerate possible activation states of all neurons by repeating $2^{\sum_{i=0}^{L-1} n_i}$ times, while for the latter, we can uniformly sample the input space by $(\frac{1}{\epsilon})^d$ times, where ϵ is the needed sampling interval, to identify the actual collective states of all neurons. As highlighted earlier, the collective activation states \mathbf{C} lead to a group of inequalities, corresponding to a polytope. We can solve all vertices of the polytope with the vertex enumeration algorithm⁴ [Avis and Fukuda, 1992] to find all vertices of a polytope. The complexity of the vertex enumeration algorithm scales linearly with the number

⁴<https://pypi.org/project/pypomant/>

of inequalities. Then, Delaunay triangulation [Chapter 23, [Toth et al., 2017]] is executed for these vertices to see how many non-overlapping simplices these vertices can gain. Lastly, we count the #simplices. Sometimes, one may not need to compute all polytopes of a neural network. Instead, the polytopes related to data are sufficient. For example, in the training-free NAS experiment [Chen et al., 2021], the authors exhausted all training data and identify associated unique polytopes.

B Average Number of Faces in Linear Regions of Neural Networks

B.1 Initialization

Proof of Theorem 1. By Theorem 6, we obtain that the number of simplices in triangulations of polytopes generated by \mathcal{N} is at most $\#\text{simplices} \leq 2n \sum_{i=0}^{d-1} \binom{n-1}{i} + 2d \sum_{i=0}^{d-1} \binom{n}{i}$. We know that the number of $(d-1)$ -dim faces is no more than the number of simplices. On the other hand, since the n hidden neurons are in general position and B is large enough, we obtain that the total number of polytopes (i.e., linear regions) produced by \mathcal{N} is $\sum_{i=0}^d \binom{n}{i}$. Therefore, the average number of faces in linear regions of \mathcal{N} is at most

$$\frac{2n \sum_{i=0}^{d-1} \binom{n-1}{i} + 2d \sum_{i=0}^{d-1} \binom{n}{i}}{\sum_{i=0}^d \binom{n}{i}} \leq \frac{2n \sum_{i=0}^{d-1} \binom{n-1}{i} + 2d \sum_{i=0}^{d-1} \binom{n}{i}}{\sum_{i=0}^{d-1} \binom{n}{i+1}}. \quad (10)$$

For each $0 \leq i \leq d-1$, we have

$$\begin{aligned} \frac{2n \cdot \binom{n-1}{i} + 2d \binom{n}{i}}{\binom{n}{i+1}} &\leq 2(i+1) + \frac{2d(i+1)}{n-i} = 2(i+1) \left(1 + \frac{d}{n-i}\right) \\ &\leq 2d \left(1 + \frac{d}{n-d+1}\right). \end{aligned}$$

Therefore, when n is large enough, we have the average number of faces in linear regions of \mathcal{N} is at most $2d + \mathcal{O}(\frac{1}{n}) \leq 2d + 1$. \square

Let $\#\mathcal{A}$ be the number of hyperplanes in an arrangement \mathcal{A} and $\text{rank}(\mathcal{A})$ be the dimension of the space spanned by the normal vectors of the hyperplanes in \mathcal{A} . An arrangement \mathcal{A} is called *central* if $\bigcap_{H \in \mathcal{A}} H \neq \emptyset$. Then we have the following results.

Lemma 1 (Theorems 2.4 and 2.5 from Stanley [2004]). *Let \mathcal{A} be an arrangement in an n -dimensional vector space. Then we have*

$$r(\mathcal{A}) = \sum_{\substack{\mathcal{B} \subseteq \mathcal{A} \\ \mathcal{B} \text{ central}}} (-1)^{\#\mathcal{B} - \text{rank}(\mathcal{B})}.$$

Lemma 2. *Let \mathcal{A} be an arrangement with m hyperplanes in \mathbb{R}^n . If all the hyperplanes in \mathcal{A} pass through the origin, and any n normal vectors of n hyperplanes in \mathcal{A} are linearly independent, then we have*

$$r(\mathcal{A}) = \binom{m-1}{n-1} + \sum_{i=0}^{n-1} \binom{m}{i}.$$

Proof. Since all the hyperplanes in \mathcal{A} pass through the origin, then the intersection of all hyperplanes in \mathcal{A} is not empty, thus each $\mathcal{B} \subseteq \mathcal{A}$ must be central. Since any n normal vectors of n hyperplanes in \mathcal{A} are linearly independent, we have

$$\text{rank}(\mathcal{B}) = \min\{n, \#\mathcal{B}\}.$$

Therefore, by Lemma 1 we obtain

$$\begin{aligned} r(\mathcal{A}) &= \sum_{\substack{\mathcal{B} \subseteq \mathcal{A} \\ \mathcal{B} \text{ central}}} (-1)^{\#\mathcal{B} - \text{rank}(\mathcal{B})} \\ &= \sum_{i=0}^n \binom{m}{i} + \sum_{i=n+1}^m (-1)^{i-n} \binom{m}{i} \\ &= \binom{m-1}{n-1} + \sum_{i=0}^{n-1} \binom{m}{i}. \end{aligned}$$

\square

By Lemma 2 we can derive the proof of Theorem 3.

Proof of Theorem 3. Since all the biases of \mathcal{N} are equal to zero, then all the hyperplanes produced by the hidden neurons pass through the origin. Assume that the number of such hyperplanes is n and they form an arrangement \mathcal{A} . Then by Lemma 2 we obtain

$$\begin{aligned} r(\mathcal{A}) &= \binom{n-1}{d-1} + \sum_{i=0}^{d-1} \binom{n}{i} \\ &= \frac{2}{(d-1)!} n^{d-1} + \mathcal{O}(n^{d-2}). \end{aligned}$$

On the other hand, for each $H \in \mathcal{A}$, it will be intersected by other $n-1$ hyperplanes in \mathcal{A} . This will produce $n-1$ hyperplanes in H , thus by Lemma 2, it will divide H into $\frac{2}{(d-2)!} n^{d-2} + \mathcal{O}(n^{d-3})$ pieces since H is a $(d-1)$ -dim hyperplane. Similarly, for each hyperplane in the boundary of $C(d, B)$, it will be divided into $\frac{1}{(d-1)!} n^{d-1} + \mathcal{O}(n^{d-2})$ pieces by n hyperplanes in \mathcal{A} . Therefore, the total number of faces of linear regions formed by \mathcal{A} is at most

$$2n \cdot \frac{2}{(d-2)!} n^{d-2} + 2d \cdot \frac{1}{(d-1)!} n^{d-1} + \mathcal{O}(n^{d-2}),$$

which is equal to

$$\left(\frac{4}{(d-2)!} + \frac{2d}{(d-1)!} \right) n^{d-1} + \mathcal{O}(n^{d-2}).$$

Finally, the average number of faces in linear regions of \mathcal{N} is at most

$$\frac{\left(\frac{4}{(d-2)!} + \frac{2d}{(d-1)!} \right) n^{d-1} + \mathcal{O}(n^{d-2})}{\frac{2}{(d-1)!} n^{d-1} + \mathcal{O}(n^{d-2})},$$

which is

$$3d - 2 + o(1) < 3d - 1.$$

□

B.2 After Training: Low-Rank

Proof of Theorem 2. When $d = 2$, the average number of faces can be naturally bounded. Let us start with a quadrilateral and add lines to it, then after adding one line in some linear region, the number of regions increases by 1 and the total number of edges increases by at most 4, thus the total number of edges is at most 4 times the number of linear regions, thus the average edge number is at most 4 for the case $d = 2$. □

Similar to the proof of Theorem 3, we can give the proof of Theorem 4 below.

Proof of Theorem 4. Similar to the proof of Theorem 3, the total number of faces of linear regions formed by \mathcal{A} is at most

$$\left(\frac{4}{(d_0-2)!} + \frac{2d}{(d_0-1)!} \right) n^{d_0-1} + \mathcal{O}(n^{d_0-2}).$$

Finally, the average number of faces in linear regions of \mathcal{N} is at most

$$\frac{\left(\frac{4}{(d_0-2)!} + \frac{2d}{(d_0-1)!} \right) n^{d_0-1} + \mathcal{O}(n^{d_0-2})}{\frac{2}{(d_0-1)!} n^{d_0-1} + \mathcal{O}(n^{d_0-2})},$$

which is

$$2d_0 - 2 + d + o(1) < 2d_0 + d - 1.$$

□

Similar to the proof of Theorem 1, we present the proof of Theorem 5 below.

Proof of Theorem 5. Similar to the proof of Theorem 1, we obtain that the number of simplices in triangulations of polytopes generated by \mathcal{N} is at most $\#\text{simplices} \leq 2n \sum_{i=0}^{d_0-1} \binom{n-1}{i} + 2d \sum_{i=0}^{d_0-1} \binom{n}{i}$. Also, the total number of polytopes produced by \mathcal{N} is $\sum_{i=0}^{d_0} \binom{n}{i}$ since any d_0 hyperplanes generated by any d_0 hidden neurons are in general position. Therefore, the average number of faces in linear regions of \mathcal{N} is at most

$$\frac{2n \sum_{i=0}^{d_0-1} \binom{n-1}{i} + 2d \sum_{i=0}^{d_0-1} \binom{n}{i}}{\sum_{i=0}^{d_0} \binom{n}{i}} \leq \frac{2n \sum_{i=0}^{d_0-1} \binom{n-1}{i} + 2d \sum_{i=0}^{d_0-1} \binom{n}{i}}{\sum_{i=0}^{d_0-1} \binom{n}{i+1}}. \quad (11)$$

For each $0 \leq i \leq d_0 - 1$, we have

$$\frac{2n \cdot \binom{n-1}{i} + 2d \binom{n}{i}}{\binom{n}{i+1}} \leq 2(i+1) + \frac{2d(i+1)}{n-i} \leq 2d_0 + \frac{2dd_0}{n-d_0+1}.$$

Therefore, when n is large enough, we derive that the average number of faces in linear regions of \mathcal{N} is also at most $2d_0 + \mathcal{O}(\frac{1}{n}) \leq 2d_0 + 1$, which is irrelevant to d . \square

C #Simplices as a Complexity Measure

Definition 2 (#Simplices as a complexity measure). *We define the complexity of a ReLU network as the minimum number of simplices: M that are needed to fill each and every polytope to support the piecewise linear function created by the ReLU network. The number of simplices contained by each polytope can be obtained by doing Delaunay triangulation [Chapter 23, [Toth et al., 2017]] with the vertices of each polytope.*

Now we illustrate the desirable properties of #simplices relative to #polytopes in terms of the uniqueness via modularization and network transform and being applicable to classification networks. Here, #simplices refers to the total number of simplices of a ReLU network, while #polytopes is the total number of polytopes.

• **One-to-one correspondence via modularization and network transform:** *Given constant #polytopes, are there functions which can only be approximated by ReLU FCNs with high #simplices and not low #simplices?* The answer is yes. A simplex is an elementary unit. Proposition 1 shows that an arbitrary ReLU network can be transformed into a wide network whose depth is the input dimension and width is determined by the #simplices. Therefore, as long as the support of functions represented by two networks is filled by the same #simplices, two networks can be represented by the network of the same width and depth. As such, we can define the equivalent class of networks as those with the same #simplices to cover their polytopes. In contrast, #polytopes cannot be used to rigorously define the equivalent networks because the polytopes are not elementary units. When one is told that two networks have the same #polytopes, one is still not totally sure whether two networks are equally complex.

Proposition 1 (#Simplices in network transform [Fan et al., 2020]). *Suppose that the representation of an arbitrary ReLU network is $h : [-B, B]^D \rightarrow \mathbb{R}$, and M is the minimum #simplices to cover the polytopes to support h , for any $\delta > 0$, there exists a wide ReLU network \mathbf{H} of width $\mathcal{O}[D(D+1)(2^D-1)M]$ and depth D , satisfying that*

$$m(\mathbf{x} \mid h(\mathbf{x}) \neq \mathbf{H}(\mathbf{x})) < \delta \quad (12)$$

where $m(\cdot)$ is the standard measure in $[-B, B]^D$.

• **Being applicable to classification networks:** The number of linear regions loses its efficacy when it comes to the classification network, because the number of linear regions will be equal to the number of labels regardless of how many distinct regions the original network has. As shown in Figure 7, two networks (2-6-1 and 2-3-1) are used to classify two concentric rings. We plot the linear regions and classification regions for two networks, respectively. Regarding classification regions, one network uses three neurons to define a triangle domain, while the other has six neurons to form a hexagon. Although the six-neuron network is apparently more complex than the other, the two networks have the same number of classification regions. However, when taking the number of simplices as the complexity measure, one can favorably avoid this counterexample. This is because the number of simplices is dependent on the number of vertices, and the number of vertices is robust in classification networks. We count the number of simplices for classification regions of two networks as 4 and 6, which agrees with the complexity of the two networks.

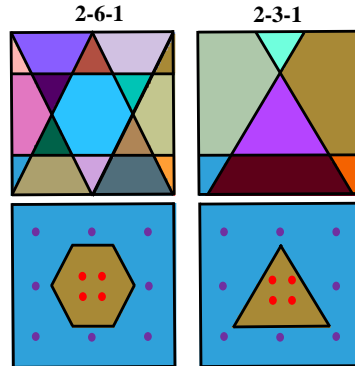


Figure 7: Model complex measure: the number of linear regions vs the number of simplices.

D Estimation to the Maximum #Simplices

Theorem 6 (Upper Bound). *Let \mathcal{N} be a feedforward ReLU NN with d input features and L hidden layers with n hidden neurons in each layer (with or without skip connections between different layers). Then the number of simplices in triangulations of all polytopes generated by \mathcal{N} is at most*

$$\frac{2n^{dL}}{(d-1)!(d!)^{L-1}} + \mathcal{O}(n^{dL-1}). \quad (13)$$

In particular, if $L = 1$, we derive the following upper bound for the maximum number of simplices

$$\#\text{simplices} \leq 2n \sum_{i=0}^{d-1} \binom{n-1}{i} + 2d \sum_{i=0}^{d-1} \binom{n}{i}.$$

Theorem 7 (Lower Bound). *Let \mathcal{N} be a multi-layer fully-connected ReLU NN with d input features and L hidden layers with n neurons in each layer. Then the maximum number of simplices in triangulations of polytopes generated by \mathcal{N} is at least*

$$\frac{n^{dL}}{d^{d(L-1)}d!} + \mathcal{O}(n^{dL-1}).$$

Furthermore, if $L = 1$, we derive the following tighter lower bound for the maximum number of simplices

$$\#\text{simplices} \geq \frac{2n}{d+1} \sum_{i=0}^{d-1} \binom{n-1}{i}.$$

It is straightforward to see $(d-1)!(d!)^{L-1} < d^{d(L-1)}d!$; therefore, the above upper bound is strictly higher than the lower bound. The basic idea to derive the above upper bound depends on the following observation: for each $(d-1)$ -dim face of a d -dim polytope, it can only be a face for one unique simplex in a triangulation of this polytope, thus the total number of simplices in triangulations of polytopes must be smaller than or equal to the total number of $(d-1)$ -dim faces in all polytopes. Therefore, we just need to derive the upper bound for the total number of $(d-1)$ -dim faces in all polytopes generated by a neural network \mathcal{N} , which can be done by induction on the number of layers of \mathcal{N} . For the lower bound, we use the fact that each d -simplex with dimension d has $d+1$ faces, thus the number of simplices should be at least the total number of $(d-1)$ -dim faces in all polytopes divided by $d+1$.

Our method to transfer the problems of calculating the above number of simplices to calculating the total number of $(d-1)$ -dim faces in all polytopes is very versatile, and thus can be applied to many complicated architectures such as fully-connected NNs, CNNs, and ResNets He et al. [2016]. Actually, we can always calculate the total number of faces in all polytopes layer by layer, by considering each face and finding out how many new faces it is divided into by new hyperplanes from the next layer.

D.1 Preliminary

Let's recall some basic knowledge on hyperplane arrangements [Stanley et al., 2004]. Let V be a Euclidean space. A hyperplane in the Euclidean space $V \simeq \mathbb{R}^n$, is a subspace $H := \{X \in V : \alpha \cdot X = b\}$, where $\mathbf{0} \neq \alpha \in V$, $b \in \mathbb{R}$ and " \cdot " denotes the inner product. A *region* of an arrangement $\mathcal{A} = \{H_i \subset V : 1 \leq i \leq m\}$ is just a connected component in the complement set of the union of all hyperplanes in the arrangement \mathcal{A} . Let $r(\mathcal{A})$ be the number of regions for an arrangement \mathcal{A} . Also, a *simplex* in an n -dimensional Euclidean space is just a n -dimensional polytope that is the convex hull of $n+1$ vertices. For example, a triangle is a simplex in \mathbb{R}^2 , and a tetrahedron is a simplex in \mathbb{R}^3 . A *triangulation* on some polytope is a division of the polytope into simplices.

The following Zaslavsky's Theorem is very crucial in the estimation of the number of linear regions.

Lemma 3 (Zaslavsky's Theorem [Zaslavsky, 1975, Stanley et al., 2004]). *Let \mathcal{A} be an arrangement with m hyperplanes in \mathbb{R}^n . Then, the number $r(\mathcal{A})$ of regions for the arrangement \mathcal{A} satisfies*

$$r(\mathcal{A}) \leq \sum_{i=0}^n \binom{m}{i}. \quad (14)$$

Furthermore, the above equality holds iff \mathcal{A} is in general position Stanley [2004].

D.2 Main results - One Layer ReLU NNs

Throughout this paper, we always assume that the input space of an NN is a d -dimensional hypercube $C(d, B) := \{\mathbf{x} = (x_1, x_2, \dots, x_d) \in \mathbb{R}^d : -B \leq x_i \leq B\}$ for some large enough constant B . Note that for a one-layer fully-connected ReLU NN, the pre-activation of each hidden neuron is an affine linear function of input values. Based on the sign of the pre-activation, each hidden neuron produces a hyperplane that divides the input space into two linear regions. On the other hand, the d -dimensional hypercube $C(d, B)$ has $2d$ hyperplanes in its boundary.

Theorem 8. *Let \mathcal{N} be a one-layer feedforward ReLU NN with d input features and n hidden neurons. Then the number of simplices in triangulations of polytopes generated by \mathcal{N} is at most*

$$2n \sum_{i=0}^{d-1} \binom{n-1}{i} + 2d \sum_{i=0}^{d-1} \binom{n}{i}.$$

Proof. Let H_1, H_2, \dots, H_n be the n hyperplanes generated by n hidden neurons and $H_{n+1}, H_{n+2}, \dots, H_{n+2d}$ be the $2d$ hyperplanes in the boundary of $C(d, B)$. Then for each $1 \leq i \leq n$, the hyperplane H_i may be intersected by other $n-1$ hyperplanes in H_1, H_2, \dots, H_n . This will produce at most $n-1$ hyperplanes in H_i , thus by Theorem 3, it will divide H_i into at most $\sum_{i=0}^{d-1} \binom{n-1}{i}$ pieces since H_i is a $(d-1)$ -dim hyperplane. Also, for each $1 \leq i \leq 2d$, the hyperplane H_{n+i} may be intersected by H_1, H_2, \dots, H_n . This will produce at most n $(d-2)$ -dim hyperplanes in H_{n+i} , thus by Theorem 3, it will divide H_i into at most $\sum_{i=0}^{d-1} \binom{n}{i}$ pieces since H_i is a $(d-1)$ -dim hyperplane. Moreover, each piece could be a face of two linear regions, finally we will get at most

$$2n \sum_{i=0}^{d-1} \binom{n-1}{i} + 2d \sum_{i=0}^{d-1} \binom{n}{i}$$

faces for all the polytopes. On the other hand, each simplex in a triangulation of polytope can be corresponding to at least one face in the polytope, and each face in the polytope can be corresponding to exactly one simplex. Therefore, the total number of simplices must be smaller than or equal to the total number of faces in all polytopes. Thus we obtain that the number of simplices in triangulations of polytopes generated by \mathcal{N} is also at most

$$2n \sum_{i=0}^{d-1} \binom{n-1}{i} + 2d \sum_{i=0}^{d-1} \binom{n}{i}.$$

□

The following results give a lower bound for the maximum number of simplices in a triangulation of a one layer fully-connected ReLU NN.

Theorem 9. *Let \mathcal{N} be a one-layer fully-connected ReLU NN with d input features and n hidden neurons. If n corresponding hyperplanes are in general position and $C(d, B)$ is large enough, then the number of simplices in a triangulation of polytopes among all n corresponding hyperplanes is at least*

$$\frac{2n}{d+1} \sum_{i=0}^{d-1} \binom{n-1}{i} = \frac{2n^d}{(d+1)(d-1)!} + \mathcal{O}(n^{d-1}).$$

Proof. Let H_1, H_2, \dots, H_n be n hyperplanes generated by n hidden neurons. Then for each $1 \leq i \leq n$, the hyperplane H_i will be intersected by other $n-1$ hyperplanes in H_1, H_2, \dots, H_n . This will produce exact $n-1$ hyperplanes in H_i since H_1, H_2, \dots, H_n are in general position, thus by Theorem 3, it will divide H_i into exact $\sum_{i=0}^{d-1} \binom{n-1}{i}$ pieces since H_i is a $(d-1)$ -dim hyperplane. When $C(d, B)$ is large enough, we can assume that every such a piece has a non-empty intersection with $C(d, B)$. Therefore, the total sum of number of $(d-1)$ -faces of all linear regions (polytopes) will be at least $2n \sum_{i=0}^{d-1} \binom{n-1}{i}$ since every piece is counted twice. On the other hand, every d -dim simplex has $d+1$ distinct $(d-1)$ -dim faces, thus every triangulation with N simplices will contain

$N(d+1)$ number $(d-1)$ -dim faces. Therefore, if a triangulation of all linear regions (polytopes) of \mathcal{N} contains N simplices, then

$$N(d+1) \geq 2n \sum_{i=0}^{d-1} \binom{n-1}{i}$$

and thus

$$N \geq \frac{2n}{d+1} \sum_{i=0}^{d-1} \binom{n-1}{i}.$$

Finally, we derive that a triangulation of all linear regions (polytopes) of \mathcal{N} contains at least $\frac{2n}{d+1} \sum_{i=0}^{d-1} \binom{n-1}{i} = \frac{2n^d}{(d+1)(d-1)!} + \mathcal{O}(n^{d-1})$ simplices. \square

D.3 Main results - Multi-Layer ReLU NNs

To study the multi-layer NNs, we need the following results from [Montúfar, 2017, Proposition 3].

Lemma 4 (Montúfar [2017]). *Let \mathcal{N} be a multi-layer fully-connected ReLU NN with d input features and L hidden layers with n_1, n_2, \dots, n_L hidden neurons. Then the number of polytopes of \mathcal{N} is at most $\prod_{i=1}^L \sum_{j=0}^{m_i} \binom{n_i}{j}$, where $m_i = \min\{d, n_1, n_2, \dots, n_i\}$.*

Theorem 10. *Let \mathcal{N} be a multi-layer feedforward ReLU NN with d input features and L hidden layers with n hidden neurons in each layer (with or without skip connections between different layers). Then the number of simplices in triangulations of polytopes generated by \mathcal{N} is at most*

$$\frac{2n^{dL}}{(d-1)!(d!)^{L-1}} + \mathcal{O}(n^{dL} - 1). \quad (15)$$

Proof. First, we prove by induction that the total number of faces generated by \mathcal{N} is at most

$$\frac{2n^{dL}}{(d-1)!(d!)^{L-1}} + \mathcal{O}(n^{dL} - 1).$$

The case $L = 1$ is proved in Theorem 8. When $L \geq 2$, we assume that Eq. (15) holds for $L - 1$. Thus by Lemma 4, and the induction hypothesis, the network \mathcal{N}' with the first $L - 1$ layers already has

$$\frac{n^{d(L-1)}}{(d!)^{L-1}} + \mathcal{O}(n^{d(L-1)-1})$$

linear regions and

$$\frac{2n^{d(L-1)}}{(d-1)!(d!)^{L-2}} + \mathcal{O}(n^{d(L-1)-1})$$

faces for all polytopes. Then when we add the L -th layer, for each polytope R with f_R faces in \mathcal{N}' , the n neurons and the f_R faces create at most $n + f_R$ hyperplanes in R (with or without skip connections between different layers, since the skip connections will not create more hyperplanes or polytopes), similar to Theorem 8 these creates

$$2n \sum_{i=0}^{d-1} \binom{n-1}{i} + f_R \sum_{i=0}^{d-1} \binom{n}{i}$$

faces for all the polytopes in R . Therefore, we obtain that the total number of faces is at most

$$\begin{aligned} & 2n \sum_{i=0}^{d-1} \binom{n-1}{i} \cdot \left(\frac{n^{d(L-1)}}{(d!)^{L-1}} + \mathcal{O}(n^{d(L-1)-1}) \right) + \sum_{i=0}^{d-1} \binom{n}{i} \sum_R f_R \\ &= 2n \sum_{i=0}^{d-1} \binom{n-1}{i} \cdot \left(\frac{n^{d(L-1)}}{(d!)^{L-1}} + \mathcal{O}(n^{d(L-1)-1}) \right) \\ & \quad + \sum_{i=0}^{d-1} \binom{n}{i} \cdot \left(\frac{2n^{d(L-1)}}{(d-1)!(d!)^{L-2}} + \mathcal{O}(n^{d(L-1)-1}) \right) \\ &= \frac{2n^{dL}}{(d-1)!(d!)^{L-1}} + \mathcal{O}(n^{dL} - 1). \end{aligned}$$

Therefore, the total number of simplices must be smaller than or equal to the total number of faces in all polytopes. Thus we obtain that the number of simplices in triangulations of polytopes generated by \mathcal{N} is also at most

$$\frac{2n^{dL}}{(d-1)!(d!)^{L-1}} + \mathcal{O}(n^{dL} - 1).$$

□

On the other hand, by the following lemma it is easy to derive the maximum number of simplices in triangulations of polytopes generated by multi-layer NNs.

Lemma 5 (Montufar et al. [2014]). *Let \mathcal{N} be a multi-layer fully-connected ReLU NN with d input features and L hidden layers with n_l hidden neurons in the l -th layer. Then the maximum number of linear regions of \mathcal{N} is at least $\prod_{l=1}^{L-1} \lfloor \frac{n_l}{d} \rfloor^d \sum_{j=0}^d \binom{n_L}{j}$.*

For the lower bounds, we have the following results.

Theorem 11. *Let \mathcal{N} be a multi-layer fully-connected ReLU NN with d input features and L hidden layers with n neurons in each layer. Then the maximum number of simplices in triangulations of polytopes generated by \mathcal{N} is at least*

$$\frac{n^{dL}}{d^{d(L-1)}d!} + \mathcal{O}(n^{dL-1}).$$

Proof. By Lemma 5, the maximum number of linear regions is lower bounded by $\left(\frac{n}{d}\right)^{d(L-1)} \sum_{i=0}^d \binom{n}{i} = \frac{n^{dL}}{d^{d(L-1)}d!} + \mathcal{O}(n^{dL-1})$. Also, the number of simplices should be larger than or equal to the number of linear regions. Thus we obtain the number of simplices in a triangulation of polytopes among all n corresponding hyperplanes is at least $\frac{n^{dL}}{d^{d(L-1)}d!} + \mathcal{O}(n^{dL-1})$. □

Now, we can derive Theorems 6 and 7 in the main text.

Proof of Theorem 6. Directly by Theorems 8 and 10. □

Proof of Theorem 7. Directly by Theorems 9 and 11. □

We empirically validate our bounds in Table 1 with 4 structures. For a network structure $X-Y_1-\dots-Y_h-\dots-Y_H-1$, X represents the dimension of the input, and Y_h is the number of hidden neurons in the h -th hidden layer. For a given MLP architecture, we initialize all the parameters based on the Xavier uniform initialization. Because all network structures we validate have a limited number of neurons, we can compute polytopes and their simplices by enumerating all collective activation states of neurons, which ensures that all polytopes are identifiable. For each structure, we repeat initialization ten times to report the maximum #simplices. As shown in Table 1, the derived upper bound is compatible with the numerical results of several network structures, which verifies the correctness of our results.

Table 1: Numerically verify the correctness of the derived upper and lower bounds for the maximum #simplices.

	3-7-1	3-8-1	3-9-1	3-10-1
Upper Bounds by Theorem 6	482	686	942	1256
Enumeration Method	446	663	893	1140
Lower Bounds by Theorem 7	77	116	166	230

D.4 Comparison of Different Network Architectures

The aim of this section is to compare the maximum #simplices based on bounds obtained in Section D.2. Our conclusion is that deep NNs usually have more number of simplices than shallow NNs with the same number of parameters.

First, let's fix some notations. For two functions $f(n)$ and $g(n)$, we write $f(n) = \Theta(g(n))$ if there exists some positive constants c_1, c_2 such that $c_1g(n) \leq f(n) \leq c_2g(n)$ for all sufficiently

large n ; $f(n) = \mathcal{O}(g(n))$ if there exists some positive constant $c > 0$ such that $f(n) \leq cg(n)$ for all sufficiently large n ; and $f(n) = \Omega(g(n))$ if there exists some positive constant c such that $f(n) \geq cg(n)$ for all sufficiently large n .

The number of parameters for the fully-connected ReLU NN \mathcal{N} is easy to compute [Pascanu et al., 2013, Proposition 7].

Lemma 6. *Let \mathcal{N} be a multi-layer fully-connected ReLU NN with d input features and L hidden layers with n hidden neurons in each layer. Then the number of parameters in \mathcal{N} is $\Theta(Ln^2)$.*

Let $S_{\mathcal{N}_1}$ be the maximum number of simplices in triangulations of polytopes generated by \mathcal{N} . Now we can derive the number of simplices per parameter for deep NNs and their shallow counterparts. The following result follows directly from Lemma 6, Theorem 6 and Theorem 7.

Theorem 12. *Let \mathcal{N}_1 be a multi-layer fully-connected ReLU NN with d input features and L hidden layers with n hidden neurons in each layer, and $d = \mathcal{O}(1)$. Then \mathcal{N}_1 has $\Theta(Ln^2)$ parameters, and the ratio of $S_{\mathcal{N}_1}$ to the number of parameters of \mathcal{N}_1 is*

$$\frac{S_{\mathcal{N}_1}}{\# \text{ parameters of } \mathcal{N}_1} = \Omega\left(\frac{1}{L} \cdot \frac{n^{dL-2}}{d^{d(L-1)}d!}\right).$$

For a one-layer fully-connected ReLU NN \mathcal{N}_2 with d input features and Ln^2 hidden neurons, it has $\Theta(Ln^2)$ parameters, and the ratio for \mathcal{N}_2 is

$$\frac{S_{\mathcal{N}_2}}{\# \text{ parameters of } \mathcal{N}_2} = \mathcal{O}\left(\frac{(Ln^2)^{d-1}}{(d-1)!}\right).$$

From Theorem 12 we obtain that $\frac{S_{\mathcal{N}_1}}{\# \text{ parameters of } \mathcal{N}_1}$ grows at least exponentially fast with the depth L and polynomially fast with the width n . In contrast, $\frac{S_{\mathcal{N}_2}}{\# \text{ parameters of } \mathcal{N}_2}$ grows at most polynomially fast with the numbers L and n .

Therefore, we have that $\frac{S_{\mathcal{N}_1}}{\# \text{ parameters of } \mathcal{N}_1}$ is far larger than $\frac{S_{\mathcal{N}_2}}{\# \text{ parameters of } \mathcal{N}_2}$ when L and n are sufficiently large. Thus we conclude that fully-connected ReLU NNs usually create much more number of simplices than one-layer fully-connected ReLU NNs with asymptotically the same number of input dimensions and parameters. This result suggests that fully-connected ReLU NNs usually have much more expressivity than one-layer fully-connected ReLU NNs.

E Supplementary Experiments for Different Depths

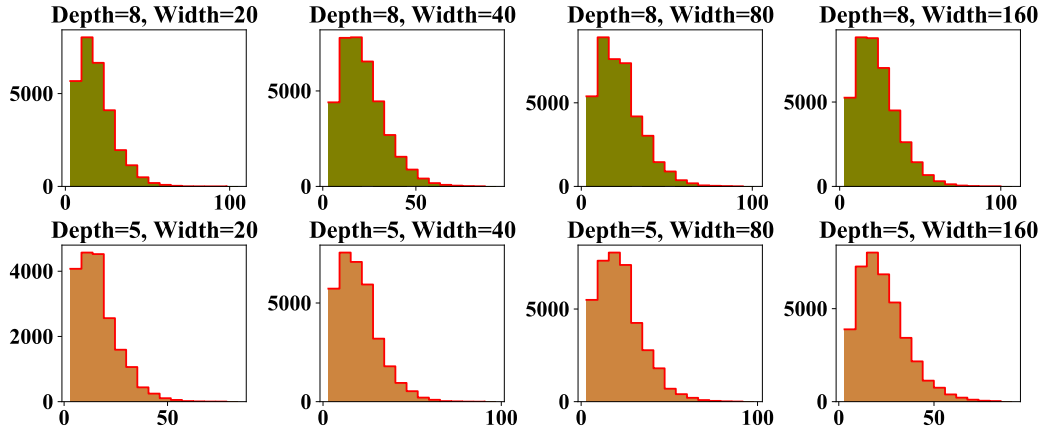


Figure 8: The uniformity and simplicity hold true for deep networks under Xavier normal initialization.

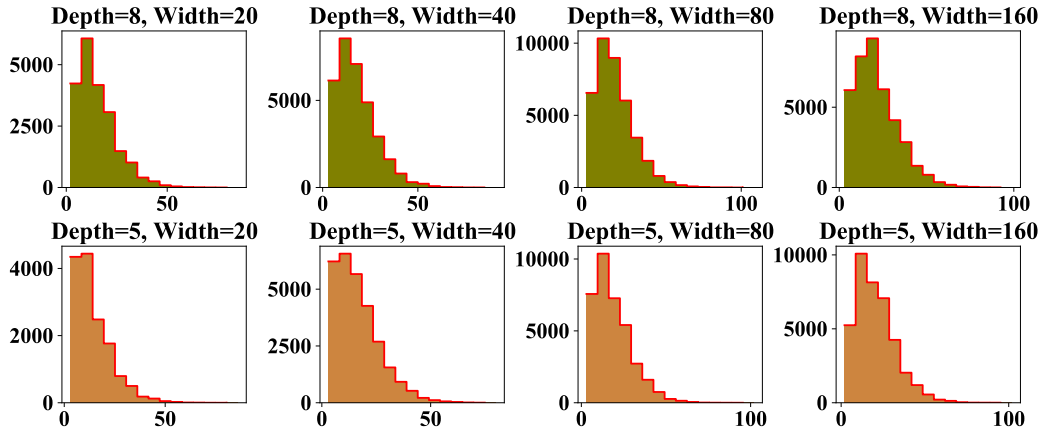


Figure 9: The uniformity and simplicity hold true for deep networks under Kaiming initialization.

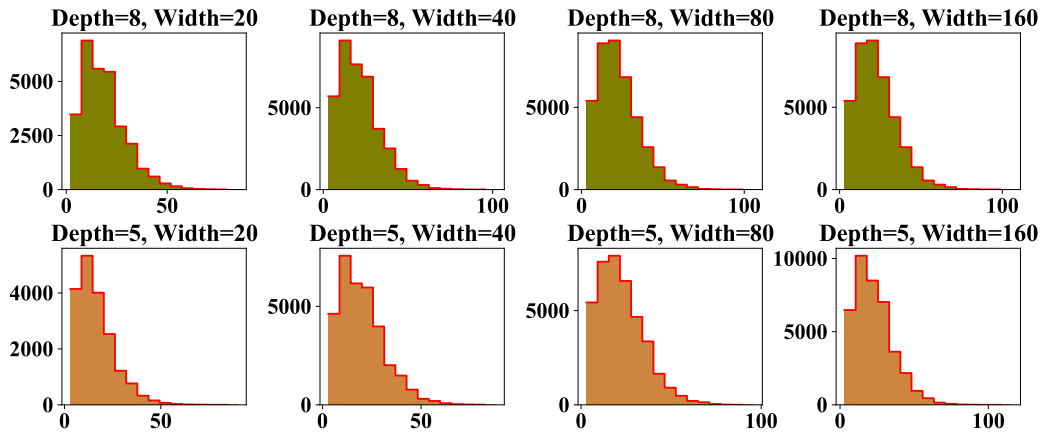


Figure 10: The uniformity and simplicity hold true for deep networks under orthogonal initialization.

F Supplementary Experiments for Much Deeper Networks

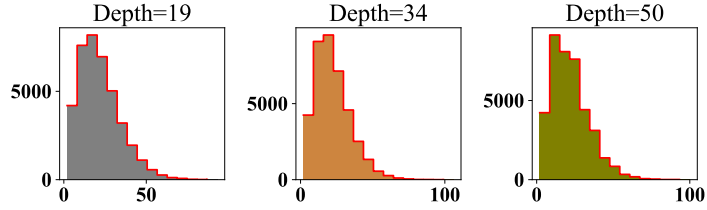


Figure 11: The simplicity and uniformity hold true for larger bounding boxes under the Xavier uniform initialization.

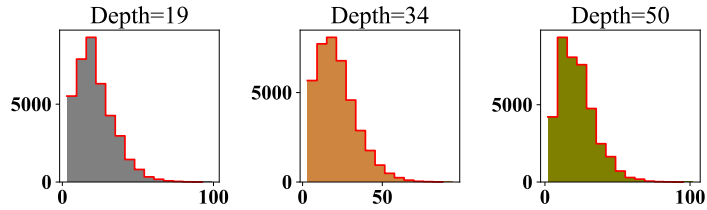


Figure 12: The simplicity and uniformity hold true for larger bounding boxes under the Xavier normal initialization.

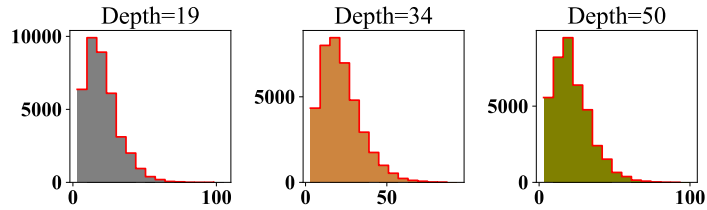


Figure 13: The simplicity and uniformity hold true for larger bounding boxes under Kaiming initialization.

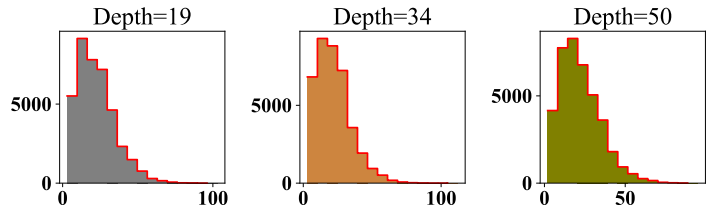


Figure 14: The simplicity and uniformity hold true for larger bounding boxes under the orthogonal initialization.

Here, we investigate if the simple polytope phenomenon holds for much deeper networks. We compute the polytopes of three networks: depth=19, depth=34, and depth=50. For all three networks, the input dimension is 3, and the width is 40. We set the bias values to 0.01. The outer bounding box is $[-1, 1]^d$, where d is the dimensionality. A total of 8,000 points are randomly sampled from $[-1, 1]^d$. At the same time, we check the activation states of all neurons to avoid computing some polytope more than once. The initialization methods are the Xavier uniform, Xavier normal, Kaiming, and orthogonal initialization. Figures 11, 12, 13, and 14 show the distribution of #simplices, from which we highlight that when the network goes deep, simple polytopes still dominate among all polytopes. Most polytopes have fewer than 25 simplices. The most complicated polytopes can have over 100 simplices.

G Supplementary Experiments for Different Biases

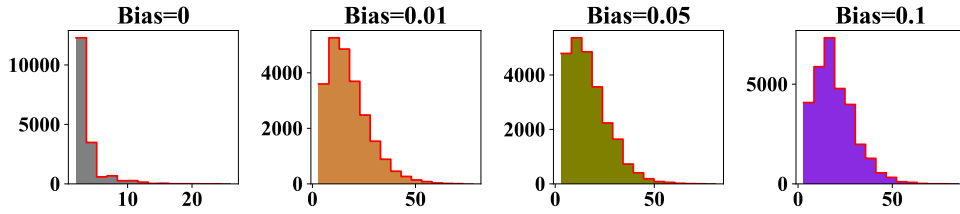


Figure 15: The simplicity and uniformity hold true for different bias values under Xavier normal initialization.

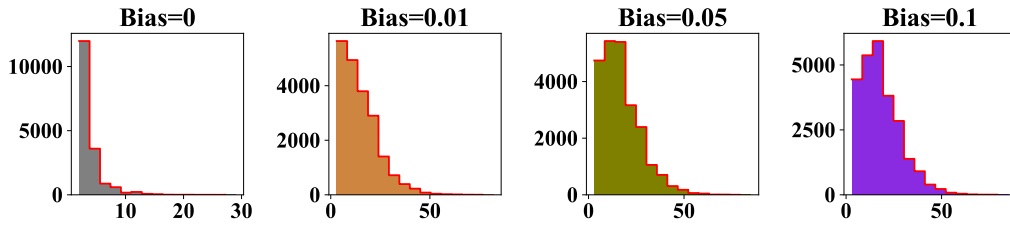


Figure 16: The simplicity and uniformity hold true for different bias values under Kaiming initialization.

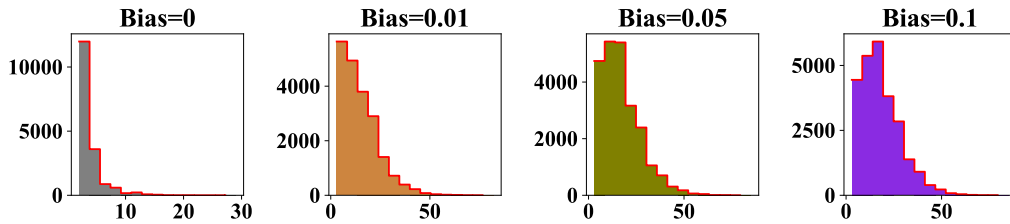


Figure 17: The simplicity and uniformity hold true for different bias values under orthogonal initialization.

H Supplementary Experiments for Bounding Boxes of Different Sizes

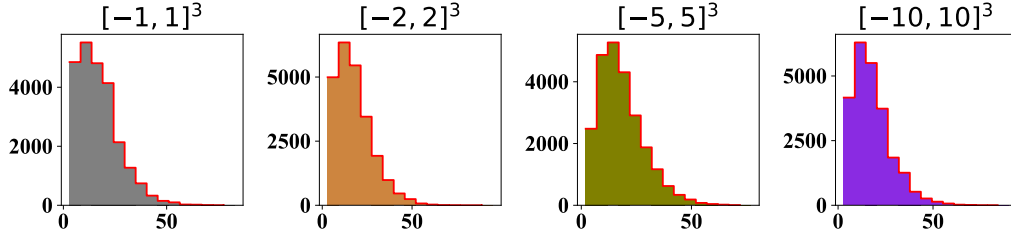


Figure 18: The simplicity and uniformity hold true for larger bounding boxes under the Xavier uniform initialization.

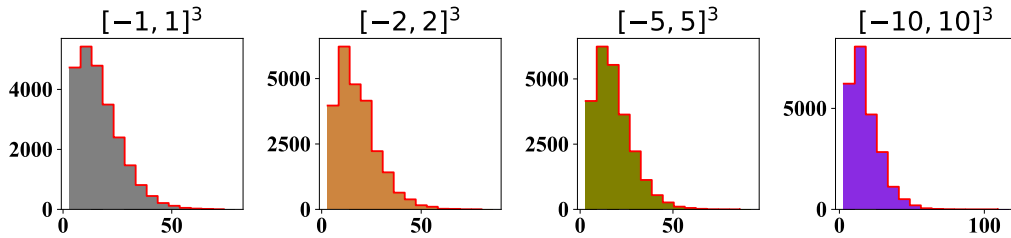


Figure 19: The simplicity and uniformity hold true for larger bounding boxes under the Xavier normal initialization.

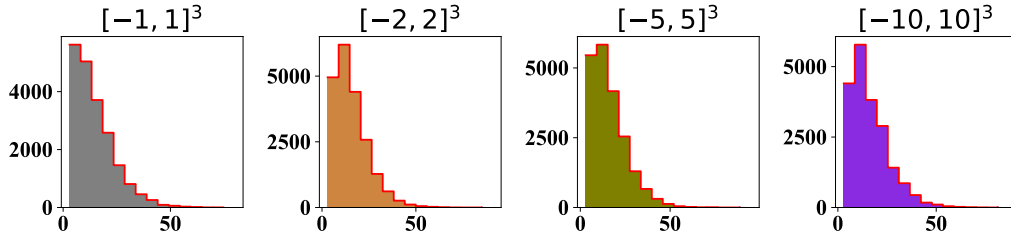


Figure 20: The simplicity and uniformity hold true for larger bounding boxes under Kaiming initialization.

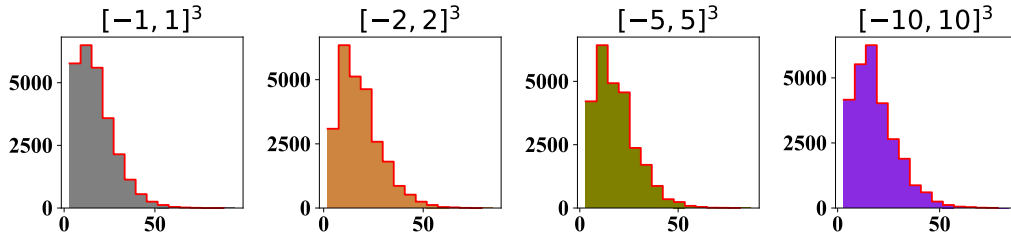


Figure 21: The simplicity and uniformity hold true for larger bounding boxes under the orthogonal initialization.

In the above experiments, we set the outer bounding box to $[-1, 1]^d$, where d is the dimension. *Will the size of the bounding box change the uniformity of linear regions?* Potentially, a larger bounding box will include more regions, and these regions may be complicated. To resolve this ambiguity, we derive the linear regions of the network 3-80-40-1 when setting the bounding box size to $[-1, 1]^3$, $[-2, 2]^3$, $[-5, 5]^3$, $[-10, 10]^3$, respectively. Earlier, we have shown that different bias

values do not affect the uniformity and simplicity of polytopes. Therefore, here we randomly set the bias value to 0.01. The initialization methods are the Xavier uniform, Xavier normal, Kaiming, and orthogonal initialization. The results are plotted in Figures 18, 19, 20, and 21, from which we have two observations. First, for different initialization methods, when the size of the outer bounding box increases, the number of polytopes increases. This is probably because more polytopes are included in the larger area. Second, we find that the uniformity and simplicity of polytopes hold for both smaller and larger bounding boxes for different initialization methods.

I Supplementary Experiments for Network Structures

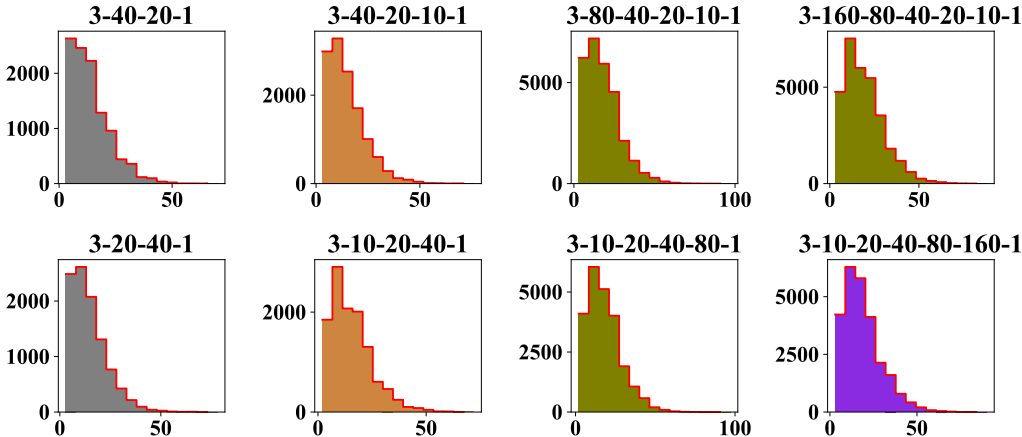


Figure 22: The simplicity and uniformity hold true for both pyramidal and inverted pyramidal structures under the Xavier uniform initialization.

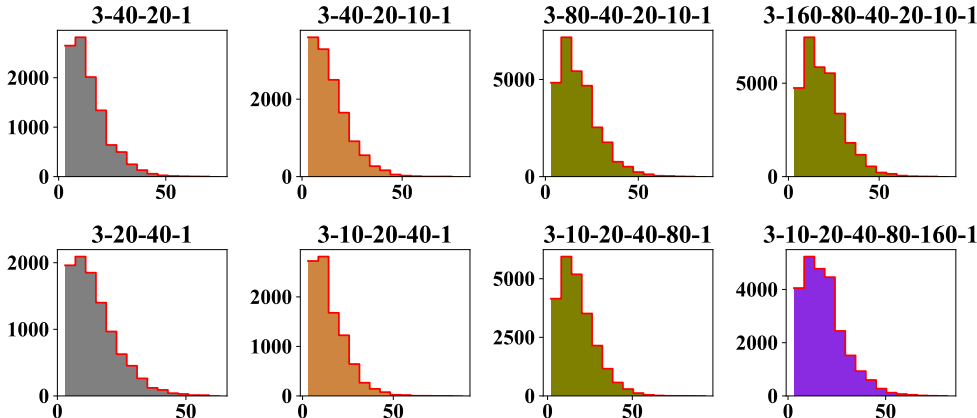


Figure 23: The simplicity and uniformity hold true for pyramidal and inverted pyramidal structures under the Xavier normal initialization.

In the above experiments, the structures of all networks we use are pyramidal. Here, we investigate how pyramidal and inverted pyramidal structures affect the uniformity and simplicity of polytopes. Earlier, we have shown that different bias values and bounding boxes do not undermine the uniformity and simplicity of polytopes. Therefore, here we randomly set the bias value to 0.01, and the bounding box size to $[-1, 1]^3$. A total of 8,000 points are uniformly sampled from $[-1, 1]^3$ to compute the polytope. At the same time, we check the activation states of all neurons to avoid counting some polytopes more than once. The initialization methods are the Xavier uniform, Xavier normal, Kaiming, and orthogonal initialization. The compared network structures are (3-40-20-1, 3-20-40-1), (3-40-20-10-1, 3-10-20-40-1), (3-80-40-20-1, 3-20-40-80-1), and (3-160-80-40-20-10-1, 3-10-20-40-80-160-1). The histograms are shown in Figures 22, 23, 24, and 25. First, we find that given the same number of neurons, for different initialization methods, the total number of polytopes generated by inverted pyramidal structures is smaller than that of pyramidal structures. This might be because a neural network is a sequential model, the earlier layer forms a basis for layer layers to cut. The earlier layers with more neurons can have more hyperplanes, which can facilitate more polytopes. Second, for different initialization methods, the uniformity and simplicity of polytopes are respected by both pyramidal and inverted pyramidal structures.

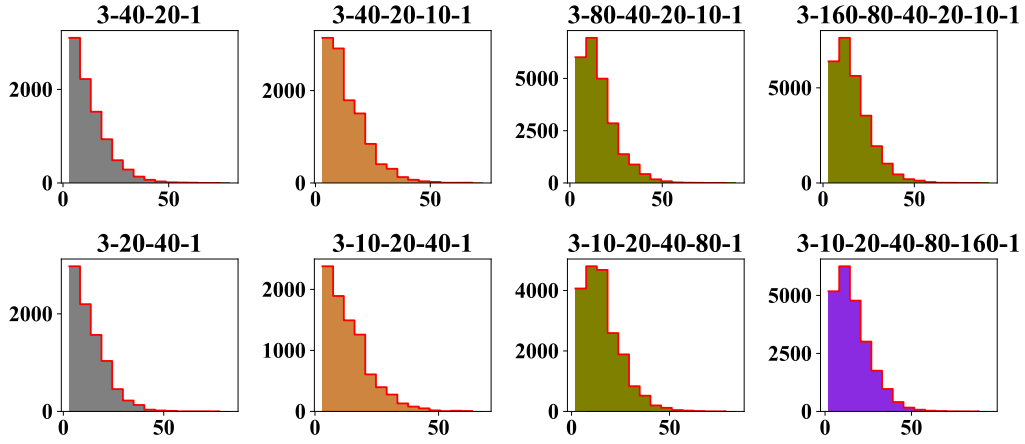


Figure 24: The simplicity and uniformity hold true for pyramidal and inverted pyramidal structures under the Kaiming initialization.

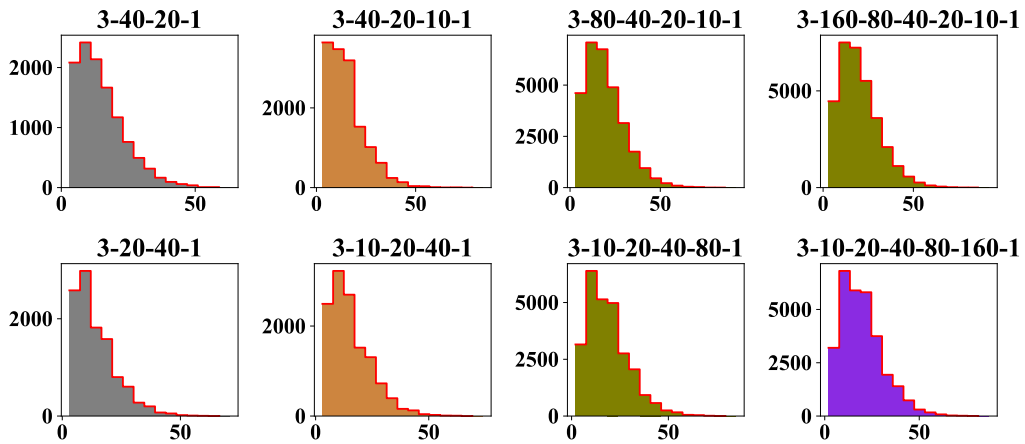


Figure 25: The simplicity and uniformity hold true for pyramidal and inverted pyramidal structures under the orthogonal initialization.

J Supplementary Experiments for Bottlenecks

Here, we investigate if the bottleneck layer in a network will affect the uniformity and simplicity of polytopes. We randomly set the bounding box size to $[-1, 1]^3$, and the bias value to 0.01. A total of 8,000 points are uniformly sampled from $[-1, 1]^3$ to compute the polytope. At the same time, we check the activation states of all neurons to avoid repetitive calculation. The initialization methods are the Xavier uniform, Xavier normal, Kaiming, and orthogonal initialization. The network structures with bottlenecks are 3-20-10-20-1, 3-20-10-10-20-1, 3-20-20-10-20-20-1, and 3-20-20-10-10-20-20-1. The histograms are shown in Figures 26, 27, 28, and 29. We find that for different initialization methods, the polytopes generated by a network with bottleneck layers are still uniform and simple.

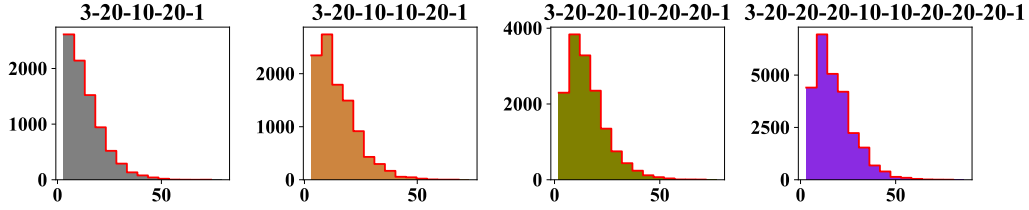


Figure 26: The simplicity and uniformity hold true for bottlenecks under Xavier initialization.

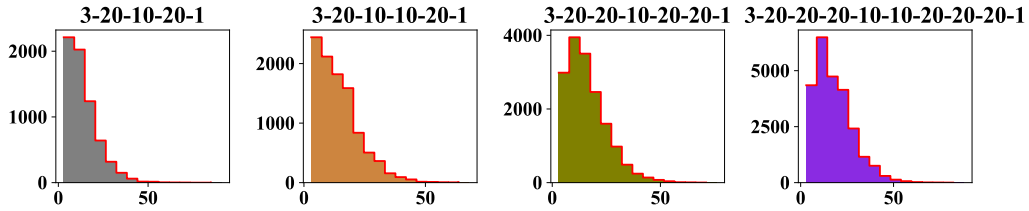


Figure 27: The simplicity and uniformity hold true for bottlenecks under the Xavier normal initialization.

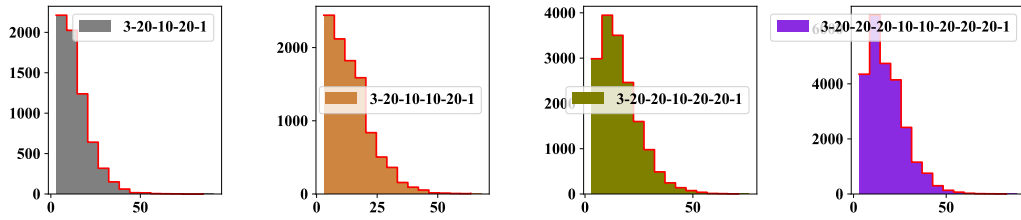


Figure 28: The simplicity and uniformity hold true for bottlenecks under the Kaiming initialization.

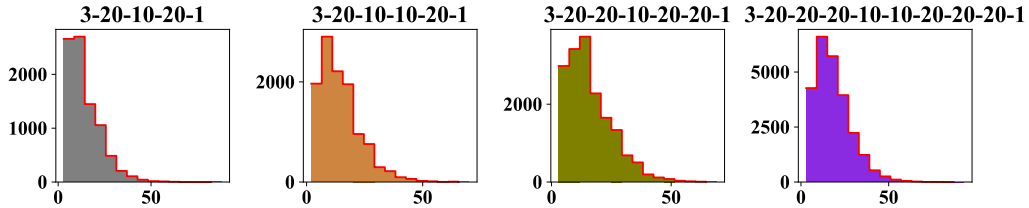


Figure 29: The simplicity and uniformity hold true for bottlenecks under the orthogonal initialization.

K Supplementary Experiments for Different dimensions

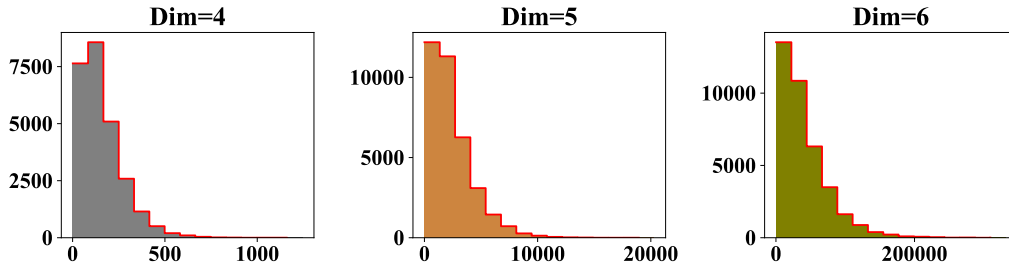


Figure 30: The simplicity and uniformity hold true for different dimensions under Xavier initialization

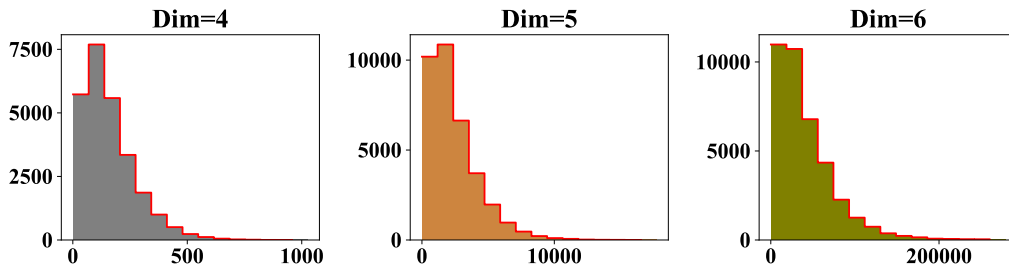


Figure 31: The simplicity and uniformity hold true for different dimensions under Xavier normal initialization

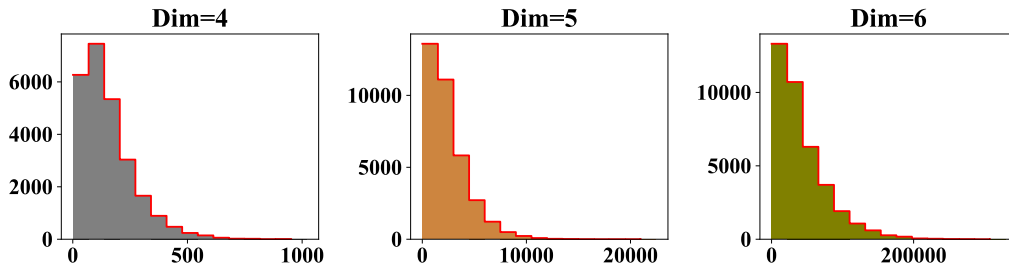


Figure 32: The simplicity and uniformity hold true for different dimensions under Kaiming initialization

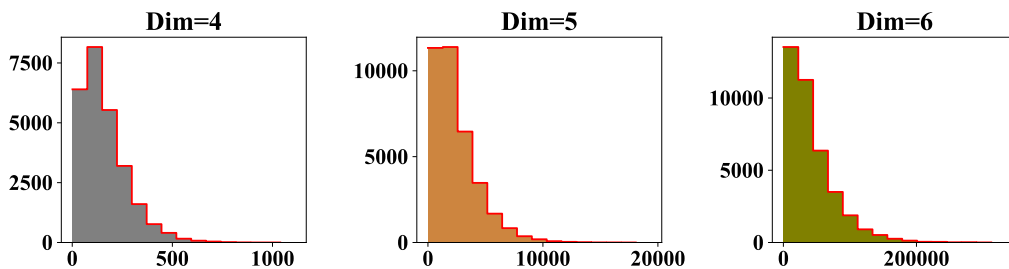


Figure 33: The simplicity and uniformity hold true for different dimensions under orthogonal initialization

Here, we investigate how the input dimension will affect the distribution of polytopes. We compute the polytopes of three networks: 4-40-20-1, 5-40-20-1, and 6-40-20-1. Due to the intrinsic difficulty of computing simplices in high dimensional space, it is very time-consuming to go higher dimensions.

We set the bias values to 0.01. The outer bounding box is $[-1, 1]^d$, where d is the dimensionality. A total of 8,000 points are randomly sampled from $[-1, 1]^d$. At the same time, we check the activation states of all neurons to avoid computing some polytope more than once. The initialization methods are the Xavier uniform, Xavier normal, Kaiming, and orthogonal initialization. Figures 30, 31, 32, and 33 show the distribution of #simplices. As the dimension increases, a polytope tends to have much more simplices, while the total number of polytopes only slightly increases. We use the triangulation method to compute the number of simplices. According to triangulation properties, the maximum number of simplices approximately equals $\mathcal{O}(M^{d/2})$, where M is the number of simplices, and d is the dimension. This is why the complexity of the linear regions will increase. For different initialization methods, most polytopes are those with a smaller number of simplices.

L Supplementary Results on the COVID Dataset Under Other Initialization

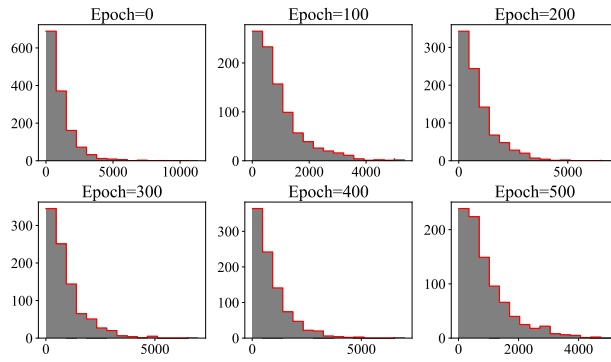


Figure 34: After training, the simplicity and uniformity hold true for Xavier normal initialization.

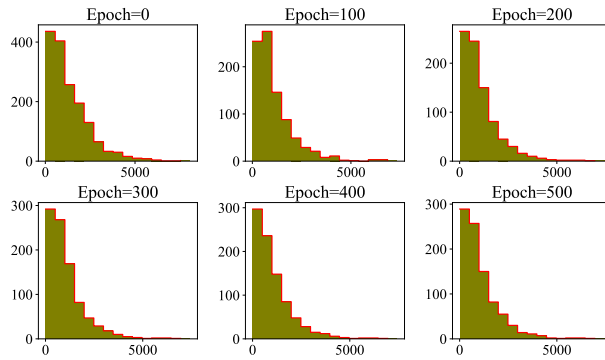


Figure 35: After training, the simplicity and uniformity hold true under Kaiming initialization.

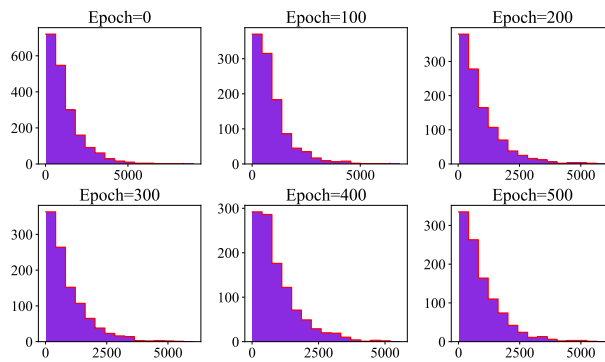


Figure 36: After training, the simplicity and uniformity hold true under orthogonal initialization.

M Estimating the Number of Faces of Polytopes by Monte Carlo Sampling

M.1 Methods

As mentioned earlier, for a fixed network and a fixed instance \mathbf{x} , $\hat{W}^{(0:l)}$ and $\hat{\mathbf{b}}^{(0:l)}$ are constant parameters uniquely determined by activation states of all neurons: $\mathbf{C} = \text{conf}(\mathbf{x})$. Furthermore, according to Eq. (3), \mathbf{C} leads to a group of inequalities:

$$(2\mathbf{c}^{(l+1)} - 1) \circ (\hat{W}^{(0:l)}\mathbf{x} + \hat{\mathbf{b}}^{(0:l)}) \geq 0, \quad l = 0, \dots, L - 1, \quad (16)$$

which encompasses a convex polytope according to the H -definition of polytopes (Chapter 16, Toth et al. [2017]). If $\text{conf}(\mathbf{x}_1) = \text{conf}(\mathbf{x}_2)$, \mathbf{x}_1 and \mathbf{x}_2 lie in the same polytope due to the uniqueness. Each inequality corresponds to a hyperplane. However, not all hyperplanes are faces of the encompassed polytope. *We call the inequalities that are faces of the encompassed polytope non-redundant inequalities.*

Although for high dimensional problems, it's difficult to find all the non-redundant inequalities (faces of a polytope) in a short time, we can, however, apply probabilistic methods to find as many as possible to provide an effective estimation. There are various probabilistic methods to find necessary linear inequalities Caron et al. [1997]. As Figure 37 shows, their basic idea is that one randomly "hits" the boundaries of the polytope from its inside. Here we simply use the classic Hit-and-Run algorithm Berbee et al. [1987]. More specifically, we use the coordinate direction method, that is, we generate random directions along each coordinate axis with equal probability.

Algorithm 2 Hit-and-Run algorithm

- 1: **Input:** $C(I), x_0 \in \text{int}(X(I))$
 - 2: $j \leftarrow 0 \quad D_0 \leftarrow \emptyset$
 - 3: **Unless** Terminating Conditions
 - 4: Generate a random direction $v_j \in B(x_j, 1)$
 - 5: **For** $i \in \{1, \dots, m\}$
 - 6: $\lambda_i \leftarrow \frac{b_i - a_i^T x_j}{a_i^T v_j}$
 - 7: $\lambda^+ \leftarrow \min_{1 \leq i \leq m} \{\lambda_i : \lambda_i > 0\}$
 - 8: $\lambda^- \leftarrow \max_{1 \leq i \leq m} \{\lambda_i : \lambda_i < 0\}$
 - 9: Denote the indices of the minimum and the maximum above as u_j^+ and u_j^- , then

$$D_{j+1} = D_j \cup \{u_j^+, u_j^-\};$$
 - 10: Generate σ from a uniform distribution on $[0, 1]$, and set

$$x_{j+1} \leftarrow x_j + (\lambda^- + \sigma(\lambda^+ - \lambda^-))v_j;$$
 - 11: $j \leftarrow j + 1$
 - 12: **output:** Indices of necessary inequities, and indices of redundant inequities D_j, ID_j
-

M.2 Experiments

We use the above method to estimate the number of faces of polytopes generated by a modified LeNet-5 trained on the MINST dataset. The modification is removing one convolutional layer and replacing all activation functions with ReLU. We randomly generate 200 instances from a uniform distribution on $[0, 1]^{28 \times 28}$. For each instance, we iteratively apply the Hit-and-Run process to detect the boundaries of the polytope containing it, and record every newly found boundaries. We set a checkpoint every 1000 iterations. Once the algorithm cannot find any new boundary in the last 1000 iterations, we consider it has found most of the boundaries of that polytope, and stop the process. The distributions of the number of boundaries we find and the number of iterations taken are shown in Figures 38 and 39. As can be seen, among 26, 796 inequalities, our algorithm finds 1, 677 boundaries on average for each polytope, with the cost of around 1.2×10^5 iterations on average. On no polytopes, our algorithm can find more than 2, 000 boundaries before reaching the stopping criteria. Therefore, this result shows that, compared with the complex structure of the network, its polytopes in fact have much fewer faces.

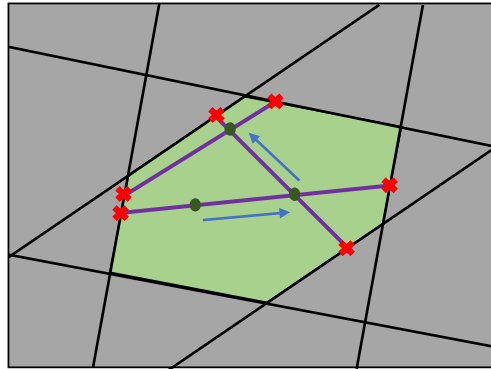


Figure 37: Hit-and-Run Algorithm

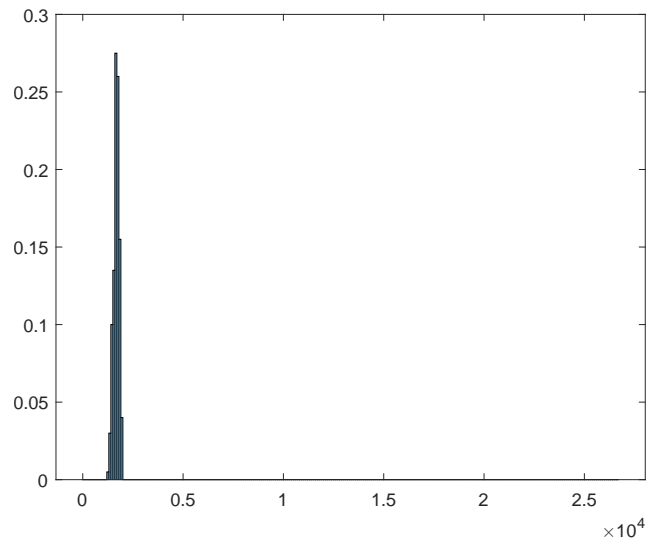


Figure 38: Distribution of Number of Boundaries Found

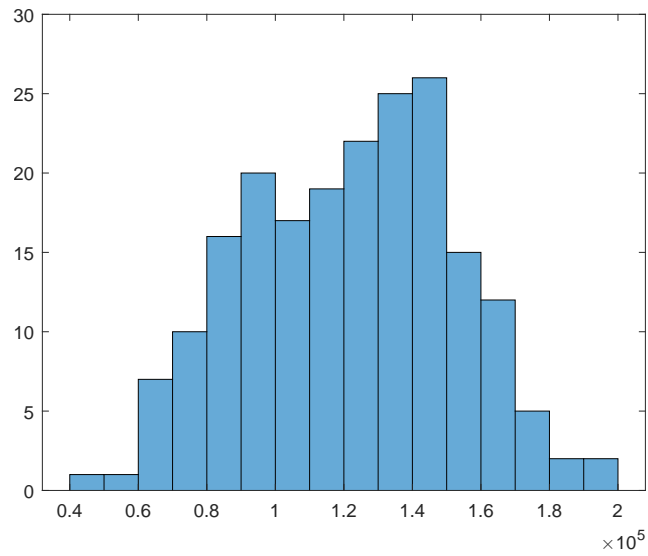


Figure 39: Distribution of Number of Iterations

N How Do Regularization Strategies Impact the Formation of Polytopes

As we mentioned, the shapes of polytopes can convey information on the mapping of a ReLU network. Here, with the number of simplices, we can provide a more quantitative approach to investigate how different regularization strategies affect a ReLU network's mapping. Let us take the weight decay as an example:

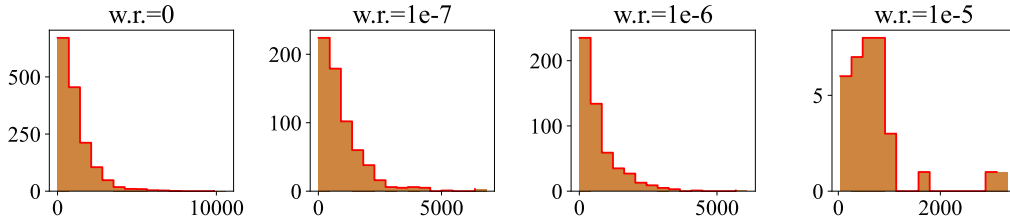


Figure 40: The pattern of how the strength of weight decay changes the complexity of polytopes under Xavier initialization.

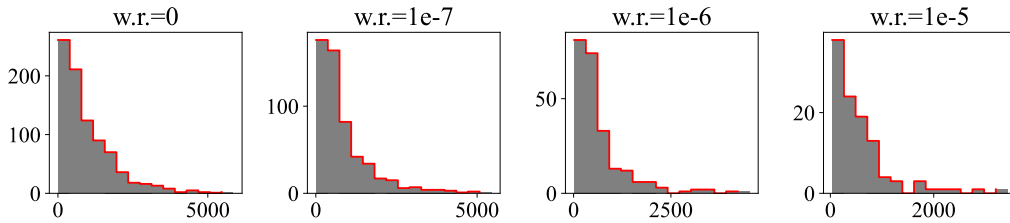


Figure 41: The pattern of how the strength of weight decay changes the complexity of polytopes under Xavier normal initialization.

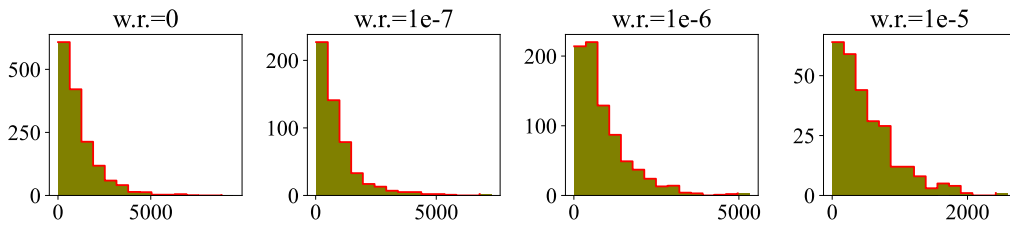


Figure 42: The pattern of how the strength of weight decay changes the complexity of polytopes under Kaiming initialization.

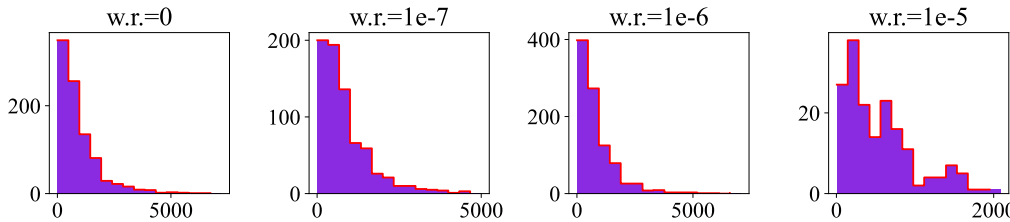


Figure 43: The pattern of how the strength of weight decay changes the complexity of polytopes under orthogonal initialization.

N.1 Weight Decay

Weight decay is a widely-used strategy to regularize the complexity of a neural network. It adds the power of all weights into the loss function to penalize the large weights. Here, we investigate how weight decay affects a ReLU network's mapping. Our natural curiosity is will the small weights tend to make simple polytopes even simpler or more complex?

Here, we follow the experimental configuration of Section 4.2. Then, we add the regularization of weight decay with the strength of 10^{-5} , 10^{-6} , 10^{-7} . The histograms of #simplices under four different initialization are shown in Figures 40, 41, 42, 43. It can be seen that when weight decay is increased, the total number of polytopes decreases for four different initialization methods. Particularly, when the weight decay is set to 10^{-5} , the total number of polytopes is dramatically smaller than that obtained without the total number of polytopes. Moreover, for the existing polytopes, their comprised simplices are fewer as the weight decay increases. Combining these observations, we summarize that weight decay can make the ReLU network learn a simpler mapping in terms of fewer polytopes and simpler polytopes.